

AD-A151 831

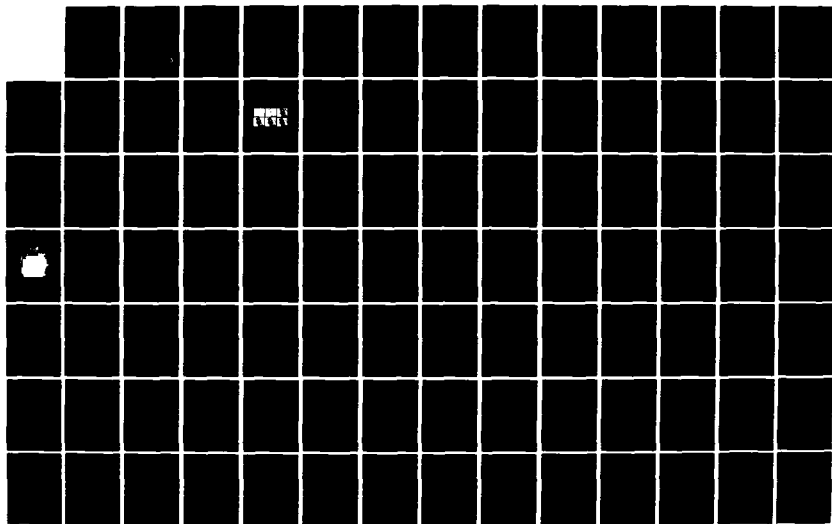
A QUANTITATIVE IMAGE EVALUATION STUDY OF A CONCURRENT
PHOTON AMPLIFICATION TREATED EMULSION(U) AIR FORCE INST
OF TECH WRIGHT-PATTERSON AFB OH K E KERN 1984
AFIT/CI/NR-85-8T

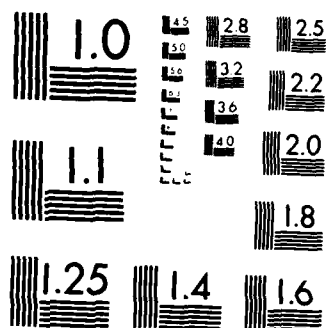
1/2

UNCLASSIFIED

F/G 14/5

NL





UNCLASS

SECURITY CLASSIFICATION OF THIS PAGE (When Data Entered)

AD-A151 831

REPORT DOCUMENTATION PAGE		READ INSTRUCTIONS BEFORE COMPLETING FORM
1. REPORT NUMBER AFIT/CI/NR 85-8T	2. SECURITY CLASS. (When Data Entered)	3. REPORT'S CATALOG NUMBER
4. TITLE (and Subtitle) A Quantitative Image Evaluation Study of a Concurrent Photon Amplification Treated Emulsion	5. TYPE OF REPORT & PERIOD COVERED ANALYSIS/DV/77/007.777007	
6. AUTHOR(s) Konrad E. Kern	7. PERFORMING ORG. REPORT NUMBER	
8. PERFORMING ORGANIZATION NAME AND ADDRESS AFIT STUDENT AT: University of Hawaii	9. CONTRACT OR GRANT NUMBER(s)	
10. CONTROLLING OFFICE NAME AND ADDRESS AFIT/NR WPAFB OH 45433	11. PROGRAM ELEMENT, PROJECT, TASK AREA & WORK UNIT NUMBERS	
12. MONITORING AGENCY NAME & ADDRESS (if different from Controlling Office)	13. REPORT DATE 1984	
	14. NUMBER OF PAGES 88	
	15. SECURITY CLASS. (of this report) UNCLASS	
16. DISTRIBUTION STATEMENT (of this Report) APPROVED FOR PUBLIC RELEASE; DISTRIBUTION UNLIMITED		
17. DISTRIBUTION STATEMENT (of the abstract entered in Block 20, if different from Report)		
18. SUPPLEMENTARY NOTES APPROVED FOR PUBLIC RELEASE: IAW AFR 190-1		
19. KEY WORDS (Continue on reverse side if necessary and identify by block number)		
20. ABSTRACT (Continue on reverse side if necessary and identify by block number) ATTACHED		

Lynn E. Wolaver
LYNN E. WOLAVER *LKW*
Dean for Research and
Professional Development
AFIT, Wright-Patterson AFB OH

DTIC
ELECTE
S **D**
MAR 27 1985
E

DD FORM 1 JAN 73 1473

85

03

11

060

SECURITY CLASSIFICATION OF THIS PAGE (When Data Entered)

A QUANTITATIVE IMAGE EVALUATION STUDY OF A
CONCURRENT PHOTON AMPLIFICATION TREATED EMULSION

by

Konrad E. Kern
B. A. University of Hawaii
(1974)

Accession For	
NTIS GRA&I	<input checked="" type="checkbox"/>
DTIC TAB	<input type="checkbox"/>
Unannounced	<input type="checkbox"/>
Justification	
By	
Distribution/	
Availability Codes	
Dist	Avail and/or Special
A-1	

A thesis submitted in partial fulfillment
of the requirements for the degree of
Master of Science in the School of
Photographic Arts and Sciences in the
College of Graphic Arts and Photography
of the Rochester Institute of Technology



July, 1984

Signature of the Author

Konrad E. Kern

Imaging and
Photographic Science

Accepted by

Paul F. Farnsworth

Coordinator, M.S. Degree Program


85 03 11 060

College of Graphic Arts and Photography
Rochester Institute of Technology
Rochester, New York

CERTIFICATE OF APPROVAL

M.S. DEGREE THESIS

The M.S. Degree Thesis of Konrad E. Kern
has been examined and approved
by the thesis committee as satisfactory
for the thesis requirement for the
Master of Science degree


Dr. Edward Granger, Thesis Advisor


Dr. William Brouwer


Maj James Mills

THESIS RELEASE PERMISSION FORM

ROCHESTER INSTITUTE OF TECHNOLOGY
COLLEGE OF GRAPHIC ARTS AND PHOTOGRAPHY

Title of Thesis: A Quantitative Image Evaluation Study of
Concurrent Photon Amplification Treated Emulsions

I, Konrad E. Kern, hereby grant permission
to the Wallace Memorial Library of R.I.T. to reproduce my thesis
in whole or in part. Any reproduction will not be for commercial
use or profit.

Konrad E. Kern

Date

29 July 84

ABSTRACT

A study was performed to evaluate the effect of concurrent photon amplification (CPA) on Kodak Tri-X Pan emulsion in regard to image quality. The study evaluated detective quantum efficiency (DQE), modulation transfer function (MTF), and information content (IC) as a function of exposure in a comparison between normal exposure and CPA.

The results showed CPA to enhance image quality relative to normal exposure at very low exposure levels. As the exposure was increased, normally exposed images became comparable and then exceeded CPA exposures in image quality. The exposure level at which normal exposure became preferential was distinct with each image quality measure.

Dedication

To God be the glory, great things he hath done,
So loved He the world that he gave us his Son.
Who yielded his life an atonement for sin,
And opened the life gate, that all may go in

Praise the LORD.....

Table of Contents

I	Introduction	1
II	Experimental	25
III	Results	40
IV	Discussion	46
V	Conclusions	54
VI	Bibliography	55
VI	Results figures	57
VII	Appencix	74
VIII	VITA	88

Table of Figures

<u>#</u>	<u>Title</u>	<u>Page</u>
1	Quantum Sensitivity Distributions	5
2	Effect of Increased Photon count on image quality	8
3	Spread function affected by flare	9
4	MTF of a system affected by flare	9
5	Line spread function output of an imaging system	17
6	Bartlett window applied to Noise data	20
7	Additivity requirement of Information	21
8	Imaging X onto Y with the addition of Noise	24
9	Edge as an array of points	27
10	Speed Graphic Camera with CPA circuit	31
11	CPA circuit Schematic	32
12	Positioning of Light Emitting Diodes	30
13	CPA Irradiance Pattern	33
14	Optical Bench Layout	34
15	Film Sensitometry	57
16	Contrast V. Log Exposure	58
17	Density Variance V. Log Exposure	59
18	DQE V. Log Exposure	60
19	M_2 V. Log Exposure, Normal Exposure	61
20	M_2 V. Log Exposure CPA Exposure	62

Table of Figures, continued

<u>#</u>	<u>Title</u>	<u>Page</u>
21	M_2 V. Log exposure, Normal and CPA regression curves	63
22	M_2 V. Log Exposure, Normal Exposure, various slit lengths	64
23	Standard deviation in M_2 measurements, various slit lengths, Normal exposure	65
24	Ratio of Good Edges, Normal exposure	66
25	M_2 V. Log Exposure, CPA Exposure, various slit lengths	67
26	Standard deviation in M_2 measurements, various slit lengths, CPA exposure	68
27	Ratio of Good Edges, CPA exposure	69
28	Edge Step Difference	70
29	Information Content V. Log Exposure, Normal Exposure	71
30	Information Content V. Log Exposure, CPA Exposure	72
31	Weiner Spectrum example	73
32	Typical point spread function	48
33	Example of adjacency effect	50

INTRODUCTION

The purpose of this section is to give a background to the experiment. The historic development and mechanism of concurrent photon amplification (CPA) will be discussed. Measures of image quality will be defined and the effect of CPA on each measure will be postulated. Finally, some measurement techniques of image quality appropriate to the laboratory will be derived or defined.

HISTORY

The development of CPA can not be attributed solely to one individual or group. In the 1930's, it was known that some additional light sensitivity in silver halide films could be gained by a slight fogging exposure near the time of the imaging exposure¹. Fogging was achieved by very briefly exposing the film to ambient light, then placing the film into the camera and making the imaging exposure. The pioneer of making the fogging exposure coincident with the imaging exposure was Cole in 1972^{2,4}. In contrast to the primitive technique of opening the film back to ambient light, Cole designed and built a device using compact electronics and light emitting diodes. His CPA device would synchronize a controlled exposure from the diodes with the operation of the shutter producing a predictable level of fogging and light sensitivity enhancement. His device was successfully marketed as a modification to a number of existing cameras and enjoyed some success among individuals interested in low light photography. To further appreciate the success of his product, an understanding of the CPA mechanism and its effect is needed.

MECHANISM

The light sensitive portion of a silver halide emulsion consists of a solution of silver halide crystals suspended in a gelatin emulsion. One photon of sufficient energy incident upon the crystal will elevate one Ag^+ ion to an Ag^0 . The Ag^0 is unstable as a singular entity and will normally revert to the Ag^+ state. However, if four or more Ag^0 appear as a localized aggregation, then all four will be stable as metallic silver. The four Ag^0 aggregate site is known as a latent image site and is capable of being a catalyst for the chemical reduction of the remainder of the crystal during development. The formation and stability of the latent image site is known as the Gurney-Mott mechanism^{1c}. The purpose of CPA is to provide a portion of those four photons generally across the emulsion. Anywhere the remaining necessary photons from the imaging exposure strike a crystal, a latent image will form.

FILM SPEED

Because fewer photons are needed during the imaging exposure, there is an apparent film speed increase. Speed increases of six stops have been reported using Tri-X Pan emulsion⁴. This represents a very significant enhancement but begs the question: What effect does CPA have on image quality? One answer is obvious, if there is an image where there was none before, there is an improvement in image quality. To evaluate that improvement, some measures of image quality must be defined or derived.

CONTRAST

The effect of CPA on contrast and the value of contrast as an image quality indicator are both very significant. The change in density vs change in log exposure is called the contrast or gamma in a photographic system. A gamma that is too low to provide an acceptable presentation of the scene content will render an unacceptable image. This is due to a certain minimum level of change in density that can be visually or instrumentally detected. A gamma equal to 1.00 is commonly desired.³ Due to the nature of film, the gamma for the mid-region of exposure will be higher than the gamma in either the toe (extreme low) or shoulder (extreme high) region of exposure. The negative deviation of gamma from this desired level degrades the image quality. CPA will tend to increase the minimum film density, thereby reducing the gamma. This effect will continue until the irradiance from the CPA device becomes insignificant compared to the scene irradiance. At that time the gamma will increase to the gamma normally held by the film.

NOISE

Noise in a photographic system is the disturbance of the image caused by the granular nature of the silver halide emulsion. A standard measure of emulsion grain noise is granularity, which is proportional to the root mean square change in density, $\sigma(\bar{D})^2$ or density variance about some mean level. This is usually measured with a small aperture densitometer at a given overall density level. The industry standard, set by Kodak, is to measure this density variance at an overall density of 1.00 with a 48 micron circular aperture scanning densitometer.⁵

If the number of photons falling upon the emulsion follow a Poisson distribution, then the distribution of the developed grains should also follow the same form. In a Poisson distribution, the variance will increase with the increasing number of developed grains. Density is defined as,

$$\text{density} = -\log(\text{transmission}), \quad (1)$$

where

$$\text{transmission} = 1 - \exp, \quad (2)$$

and \exp = the fraction of grains that are exposed. For the domain where the Poisson variance equals the number exposed and the number exposed is linearly increasing with increasing exposure, density variance will increase with increasing exposure.

The impact of CPA upon the noise level in the emulsion comes through the generation of fog. By its nature, CPA will generate an increased level of fog relative to normal exposures and by association an increase in the noise level of the emulsion. This is related to the quantum sensitivity distribution of the emulsion which is the relative number of grains that become developable. Crystals which require four photons to achieve a latent image site are said to have a quantum sensitivity of four. In this situation, CPA could provide 75% of the required irradiance to create the latent image. For crystals with a much higher quantum sensitivity, e.g., 20, CPA could provide a higher percentage of the photons necessary. Measured sensitivity distributions of various workers⁶ using special test emulsions range from a minimum level of 3 to over 20, and are shown in figure 1.

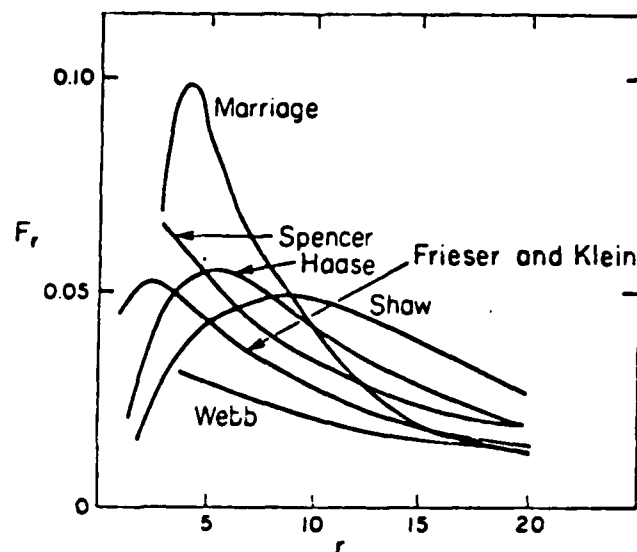


figure 1, Measured Sensitivity Distributions

These results are not contrary to the classic Gurney-Mott mechanism because these are considered probabilistic processes.

The sensitivity distribution of the emulsion shows both the potential benefit and problems of CPA. A level of CPA that would give optimum enhancement for grains requiring high quantum exposure would generate fog in grains needing low quantum exposure. The compromise is immediately apparent, the more the image is enhanced with CPA, the more fog and noise generated.

MODULATION

Modulation is defined by the equation

$$\text{modulation} = (D_{\text{max}} - D_{\text{min}}) / (D_{\text{max}} + D_{\text{min}}). \quad (3)$$

Where D_{max} is the maximum density in the region of the boundary, say the dark side of an edge. D_{min} is the minimum density on the alternate side of the boundary. CPA will raise the mean level of both D_{min} and D_{max} in a non-linear manner, therefore the overall effect is uncertain. When the change in D_{max} is greater than the change in D_{min} , there will be an improvement in modulation. However, D_{max} will reach some

ultimately limiting value and while D_{min} continues to rise, CPA will have the effect of reducing modulation. If the spatial relationship between D_{max} and D_{min} is varied, and modulation measured at each spatial frequency, the resulting plot of modulations vs spatial frequency constitutes the familiar modulation transfer function (MTF). MTF is a very valuable tool to evaluate the information carrying capability of an emulsion. A specific means of determining MTF will be discussed later.

The limit of resolution is the spatial frequency where the minimum discernable modulation occurs. This minimum discernable modulation may be determined by human or instrumental means. For both CPA and normal exposure it is possible to predict the effect of increasing exposure upon resolution in the exposure region when the change in D_{max} is greater than the change in D_{min} . A relationship can be derived between minimum discernable modulation and resolution in terms of exposure⁷. Their relation can be seen by considering two adjacent squares receiving EX1 and EX2 levels of exposure in terms of photons per area. These two squares are discernable when

$$EX1 + k(EX1)^{1/2} = EX2 - k(EX2)^{1/2}, \quad (4)$$

or

$$EX1 - EX2 = k ((EX1)^{1/2} + (EX2)^{1/2}). \quad (5)$$

The value of k used is a function of the confidence required to insure a discernable difference exists. Altman and Zweig have shown that if $k = 5$, there is a 1 part per million error rate.²¹ Therefore, k is normally set equal to 5. A higher tolerable error rate would result in a lower value of k . These two squares are considered as part of a

larger image with an overall average exposure of EX_B . Modulation is defined as

$$M = (EX_2 - EX_1)/(EX_2 + EX_1), \quad (6)$$

If,

$$EX_1 + EX_2 = 2EX_B \quad (7)$$

and

$$(EX_1)^{1/2} + (EX_2)^{1/2} = 2 (EX_B)^{1/2}. \quad (8)$$

The combination of equations 5, 7, and 8 into 6 leads to an expression for minimum discernable modulation,

$$M_{min} = k(EX_B)^{-1/2}. \quad (9)$$

If each patch has an equal area, denoted area, the resolution required to discern them, R , is equal to,

$$R = (\text{area})^{-1/2}. \quad (10)$$

The relation of equation 10 is only appropriate where the two patches are completely independent. In any real system involving lenses, chemistry, and emulsions, this relation is only valid at very low spatial frequencies.

If the average flux per area is

$$EX_B = np/\text{area},$$

where np is the absolute number of photons. Equation 10 is multiplied by unity,

$$R = (1/(EX_B)^{1/2}) (EX_B)^{1/2} / (\text{area})^{1/2}. \quad (12)$$

Using

$$M_{min}/k = (EX_B)^{-1/2}, \quad (13)$$

Equation 10 can be rewritten as

$$R = M_{min} (EX_B)^{1/2} / k. \quad (14)$$

The implicit limitation of these three factors, minimum discernable modulation, average exposure, and resolution, is due to photon noise and can be seen in figure 2⁸. The eye normally sees a time averaged or integrated level of the light. In low light photography, the interval of integration and/or number of available photons is reduced and the random nature of the photons is clearly seen. Photon noise is the ultimate lower limit of the image's ability to convey information and experimentally is inseparable from grain noise.



(a) 3×10^3 photons (b) 1.2×10^4 photons (c) 9.3×10^4 photons
 (d) 7.6×10^5 photons (e) 3.6×10^6 photons (f) 2.8×10^7 photons

Figure 2, The effect of increasing photon exposure on image quality

This derivation assumes the exposure distribution will be Poisson in nature regardless of the size of the areas considered and that each

patch, or photon detector is entirely independent. Those assumptions aside, in general the ability to resolve an object presented in the MTF of a film system should improve with increasing exposure. The relative improvement of a CPA exposed emulsion is relative to the CPA contribution to the average exposure.

There is one final consideration to apply in postulating the effect of CPA on MTF. Within a linear system, a Fourier transform of a sum is equal to the sum of the transforms. This rule is appropriate to a consideration of CPA because the resulting image is the sum of the lens induced spread and the generalized flare, or irradiance from the CPA device. The line spread function of a system affected by flare can be shown as:

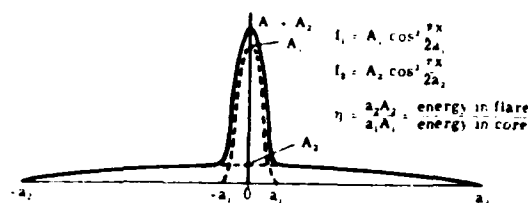


fig 3, Spread function affected by flare¹⁰

The resulting spread function is the sum of the flare and the lens induced spread. η is equal the ratio of the energy in the flare to the energy in the optic spread. The result of increasing values of η on the system MTF is shown below¹⁰:

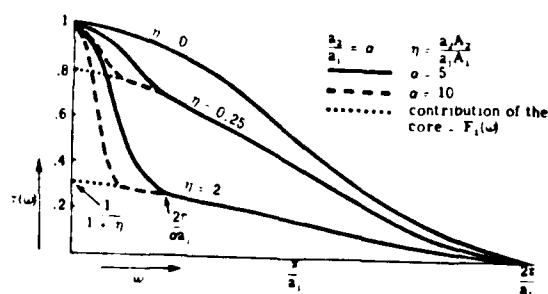


fig 4, MTF of a system affected by flare¹⁰

IMAGE QUALITY MEASUREMENTS

It is now appropriate to focus attention upon some previous image quality studies concerning CPA and discuss some measures of image quality that are available for this study.

Historically, studies of CPA effect have focussed upon the additional film speed obtained. Two image quality studies have been performed. One used resolution targets with the result that CPA didn't affect resolution in regions where normal exposure also rendered an image.⁴ A study at Rochester Institute of Technology by B.R. Desai studied the effect of CPA on detective quantum efficiency (DQE) relative to normal exposures.⁵ DQE will be derived in the next section. The result of that study was that CPA produced a better image, as measured by a higher DQE in the exposure regions where a normally exposed image was only marginally possible.

Other measures exist to evaluate image quality which will be defined or derived. Because of the historic significance of DQE, that measure will be derived and used in the study. A measure of modulation transfer function known as the second moment approximation will be derived. Wiener spectrum is a measure of the emulsion noise as a function of spatial frequency. It will be defined and incorporated into the derivation of the final measure, information content. These four measures: DQE, MTF, Wiener spectrum, and information content will yield a more comprehensive evaluation of CPA than previously performed.

DETECTIVE QUANTUM EFFICIENCY

One measure of image quality that incorporates contrast and grain

noise as a function of exposure is called DQE. An equation for DQE has been derived from a theoretical consideration of photon receptors. This derivation is excerpted from Dainty and Shaw, Image Science¹⁷. A number of assumptions are made that detract from absolute rigor in favor of reasonable application and these assumptions will be addressed at the end of the derivation.

Given an array of equal sized (area=a) independent photo receptors irradiated with an average of q photons per detector, the probability that a single detector will receive r photons is,

$$P(r) = q^r e^{-q}/r!. \quad (15)$$

For the purposes of this derivation it is assumed the detector is 100% efficient in photon absorption between a threshold level, T , and a fixed saturation level, S . Below T and above S the detector will be 0% efficient. While this detector would be impossible in reality, it roughly approximates a photographic emulsion. A photographic emulsion requires a minimum level of irradiance to achieve a density above the base + fog level. The base + fog level is that level of density inherent in the film that would be seen if the totally unexposed film were developed. Conversely, there is a maximum film density that can be achieved, after which the addition of more photons does not yield any increase in density.

In any exposure the number of detectors that will saturate is,

$$NSD = \sum_{r=S}^{\infty} q^r e^{-q}/r!. \quad (16)$$

The average count level, c_1 , is,

$$c_1 = \sum_{r=T}^{S-1} (r-T+1) q^r e^{-q}/r! + \sum_{r=S}^{\infty} DL q^r e^{-q}/r!. \quad (17)$$

where DL is the difference between saturation and threshold level plus one or $DL = S-T+1$. The equation can be simplified to,

$$c_1 = DL (1 - f_1 e^{-q}),$$

where $f_1 = 1/DL \left(\sum_{r=0}^{T-1} q^r/r! + \sum_{r=0}^T q^r/r! + \sum_{r=0}^{T+1} q^r/r! + \dots + \sum_{r=0}^{S-1} q^r/r! \right) \quad (18)$

It is necessary evaluate the gradient or change in detector count with change in input photons, which is,

$$g = d(c_1)/d(q) = DL e^{-q} (f_1 - d(f_1)/d(q)). \quad (19)$$

The summations simplify to,

$$f_2 = f_1 - d(f_1)/d(q) = 1/DL \sum_{r=T-1}^{S-1} q^r/r!. \quad (20)$$

Therefore

$$g = DL f_2 e^{-q}, \quad (21)$$

where,

$$f_2 = 1/DL \sum_{r=0}^{DL-1} q^r/r!.$$

The gradient, g , will have a value of 0 until q exceeds T and a value of unity until g approaches S , the saturation, afterwards, the gradient will fall to 0 again.

There will be a spatial distribution in the image resulting from

the statistical distribution of photons. Of interest is $d(\bar{c})^2$ or mean square fluctuations in counts. This can be calculated from the second moment of the distribution. The second moment about the mean level is equal to the second moment about the origin minus the square of the first moment.

$$d(\bar{c})^2 = m_2 = m_2' - c^2 \quad (22)$$

The first moment is simply the mean count level. The second moment about the origin, m_2' is

$$m_2' = \sum_{r=0}^{DL-1} r^2 q^r e^{-q}/r! + \sum_{r=DL}^{\infty} DL^2 q^r e^{-q}/r!. \quad (23)$$

The summations can be manipulated to yield

$$m_2' = DL^2(1 - f_3 e^{-q}),$$

where

$$f_3 = 1/DL^2 \left(\sum_{r=0}^{T-1} q^r/r! + 3 \sum_{r=0}^T q^r/r! + 5 \sum_{r=0}^{T+1} q^r/r! \dots \right. \\ \left. + (2DL-1) \sum_{r=0}^{S-1} q^r/r! \right) \quad (24).$$

Combining equations,

$$d(\bar{c})^2 = DL^2((1 - f_3 e^{-q}) - (1 - f_1 e^{-q})^2), \quad (25)$$

where f_3 is eq 24 and f_1 is eq 18.

A relation of variance in to variance out or $d(c)^2$ to $d(q)^2$ must be defined. The noise in the image is referred back to exposure,

$$d(\bar{c})^2/(d(c)/d(q))^2 = d(\bar{c})^2/q^2.$$

It is assumed the distributed photons follow a Poisson distribution, therefore,

$$d(\bar{q})^2 = q \quad (26).$$

and at exposures below saturation, the ratio of signal variance in to signal variance out is defined as DQE, where,

$$DQE = d(\bar{q})^2 / (d(\bar{c})^2 / g^2). \quad (27)$$

Assuming a Poisson relation between $d(q)^2$ and q , DQE now becomes,

$$DQE = q g / d(\bar{c})^2.$$

The ratio DQE will always be less than 1.0 because of entropy considerations. DQE can be shown to be the ratio of signal/noise into the imaging system to signal/noise out. If,

$$SNR = q / \sqrt{q} = \sqrt{q}. \quad (28)$$

Therefore, $SNR_{in}^2 = q$. By the same relation, the noise in the image is,

$$SNR_{out}^2 = d(\bar{c})^2 [d(q) / d(\bar{c})]^2 = d(\bar{c})^2 / g^2. \quad (29)$$

Therefore,

$$DQE = d(q)^2 g^2 / d(\bar{c})^2 = q g^2 / d(\bar{c})^2, \quad (30)$$

which is the ratio of the squares of SNR_{out} to SNR_{in} .

The factors of DQE: gradient, g , exposure in photons, q , and output variance $d(\bar{c})^2$ will be defined in terms of the photographic image.

In photographic systems, the image is evaluated in terms of density, which is defined as,

$$D = \log_{10}(I_0/I_t) = -\log_{10} T, \quad (31)$$

where,

I_o = irradiance out
 I_t = irradiance in
 T = transmission = I_o/I_t

If the light subtracted from I_t is proportional to the mean count level, c_l , then,

$$I_o = I_t - c_l b I_t. \quad (32)$$

where b is a fixed proportion of the incident irradiance. By substitution,

$$D = -\log_{10}(1 - c_l b), \quad (33)$$

and using the mean count level,

$$D = \log_{10}(1 - b DL(1 - f_1 e^{-q})). \quad (34)$$

In a photographic system, the gradient is defined in terms of density or $d(D)/d(f(q))$.

$$\text{Gamma} = d(D)/d(\log_{10} q). \quad (35)$$

Because,

$$d(\log_{10} q) = \log_{10} e \, d(q)/q, \quad (36)$$

$$\text{Gamma} = (q/\log_{10} e)(d(D)/d(q)), \quad (37)$$

and

$$d(D)/d(q) = \text{Gamma} \log_{10} e/q. \quad (38)$$

The scanning aperture, A , covers N of small area a , detectors, $A = Na$. Density variance is now being measured as a function of this scanning aperture size, which is referred to as $d(D_a)^2$. Likewise exposure is considered as a function of the same scanning area, giving q_a : $q_a = q/A$. The system output noise is now,

$$d(D)^2 [d(q)/d(D)] = d(D)^2 [q_a / \text{Gamma} \log_{10} e]^2. \quad (39)$$

DQE now becomes,

$$\text{DQE} = [(\log_{10} e)^2 \text{Gamma}^2] / [q_a d(D_a)^2]. \quad (40)$$

To evaluate $d(D_a)^2$, it is known that,

$$D = -\log_{10}(1 - b cl). \quad (41)$$

If the change in density with respect to change in count remains constant with area,

$$d(D)/d(cl) = b \log_{10} e / (1 - b cl) = d(D_a)/d(cl_a). \quad (42)$$

The finite fluctuations must be small enough to make this differential equation predictable. This can be done by making the scanning area, A , large enough to encompass a large number of individual detectors. The mean square fluctuation measure of A area containing N detectors will be related to the mean square fluctuation when measured for individual detectors by,

$$d(cl_a)^2 = 1/N(d(cl)^2). \quad (43)$$

Considering that $A = Na$ and combining equations,

$$A d(D_a)^2 = [a (b \log_{10} e)^2 d(cl)^2] / [1 - b cl]. \quad (44)$$

By substitution,

$$DQE = \frac{(\log_{10} e)^2 \text{Gamma}^2}{q_a A d(D_a)^2}. \quad (45)$$

This is a very effective tool for evaluating an emulsion's capacity. A , $d(\overline{D_a})^2$, Gamma , and q_a are easily measured. As previously indicated, DQE measurement has been employed in the past in a comparison of normal vs CPA exposure. A Poisson distribution viewed through a finite aperture is not rigorously Poisson and except in a highly idealized case, detectors do not possess the independence assumed in this derivation. Because of these assumptions, the material is practical but not totally rigorous.

MODULATION TRANSFER FUNCTION

In this section the basis for MTF will be defined and a simple approximation derived that will be used in the experiment. Modulation transfer function (MTF) is a tool for evaluating the relative ability of a system to transfer signal information as a function of spatial frequency. To understand MTF, a one dimensional model of the imaging system is assumed. a line function which approximates a deltafunction in one dimension is input. The output of the imaging system is the line spread function, $l(x)$, as shown below:

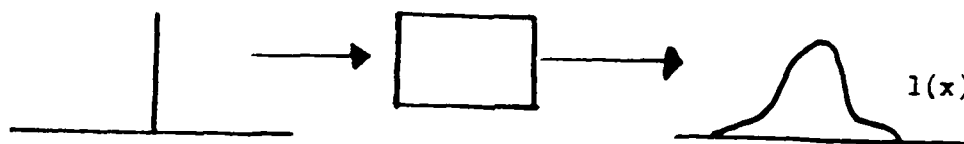


figure 5, Line spread function output of an imaging system

The optical transfer function (OTF) is the Fourier transform of the line spread function or,

$$OTF(f) = \int_{-\infty}^{\infty} l(x) e^{-i 2\pi f x} dx. \quad (46)$$

and the MTF is the modulus of the OTF or,

$$MTF(f) = |OTF(f)|. \quad (47)$$

The one dimensional model represents only a slight simplification. If a two dimensional delta function is applied to the system, the resulting impulse response function is the point spread function, $P(x,y)$. In the absence of asymmetric optical aberrations, $P(x,y)$ can be assumed to be radially symmetric about its peak. The line spread function can be

$$l(x) = d(e(x))/dx. \quad (49)$$

found by integrating the point spread function over all y ,

$$l(x) = \int P(x,y) dy. \quad (48)$$

The line spread and point spread function are difficult to generate in the laboratory. For ease, the edge function, $e(x)$ is used, created by a light/dark transition. This is related to the line spread function by,

The method of calculating MTF to be used in this study is the second moment approximation. Its benefits are simplicity and accuracy in predicting MTF to about 0.30 relative modulation.¹⁵ To calculate the second moment MTF approximation, $e^{-i2\pi fx}$ is series expanded,

$$e^{-i2\pi fx} = \sum_{n=0}^{\infty} (-i 2\pi f x)^n / n!. \quad (50)$$

Fitting this into equation 46 gives:

$$MTF(f) = \int_{-\infty}^{\infty} l(x) \sum_{n=0}^{\infty} (-2\pi f x)^n / n! dx \quad (51)$$

$$= \int_{-\infty}^{\infty} l(x) dx - i 2\pi f \int_{-\infty}^{\infty} l(x) x dx - 2\pi^2 f^2 \int_{-\infty}^{\infty} l(x) x^2 dx - \text{higher order terms}$$

(52)

Convention dictates that the area of $l(x)$ be normalized, therefore

$$\int_{-\infty}^{\infty} l(x) dx = 1.0. \quad (53)$$

The N^{th} moment of a function is given by $\int_{-\infty}^{\infty} l(x) x^N dx$ (54)

By proper choice of a coordinate system the first moment, M_1 can be set to zero and the second moment, M_2 properly computed. The equation for MTF now becomes,

$$MTF(f) = 1 - 2\pi^2 f^2 M_2. \quad (55)$$

WEINER SPECTRUM

The Wiener spectrum is a measure of the emulsion noise as a function of spatial frequency. It is a specialized application of the concept of power spectrum which may apply to either the signal or the noise in an emulsion. The Wiener-Khintchin theorem relates the image variance in the spatial domain to the spatial frequency domain. The Wiener-Khintchin⁹ theorem states that $C(x)$ and $W(f)$ are Fourier transform pairs where $C(x)$ is the auto-covariance of any function, $f(x)$

$$C(x) = \int_{-\infty}^{\infty} (f(a)-u)(f^*(a+x)-u)da. \quad (56)$$

where $f^*(a)$ is the complex conjugate of $f(a)$ and u is the mean value of the process or DC level. The transform pairs are,

$$C(x) = \int_{-\infty}^{\infty} W(f)e^{i 2\pi f x} df, \quad (57)$$

and

$$W(f) = \int_{-\infty}^{\infty} C(x)e^{-i 2\pi f x} dx. \quad (58)$$

In practice the Wiener spectrum is measured by sampling the grain noise with an elongated slit. The sampling interval, dx , of the slit in conjunction with the slit width, determines the maximum detectable frequency. The highest detectable frequency, f_{max} , is determined by

$$f_{max} = (2dx)^{-1}. \quad (59)$$

The slit width is convolved with the grain noise during the sampling process. The sampling slit width is set so that the sinc function that results from the transform of the rectangle function will experience its first zero at f_{max} . This is done by setting the slit width equal to $2dx$. The purpose of this selected slit width is to prevent aliasing during the Fourier transform process. Aliasing is the process whereby high frequency power becomes confused with low frequency power. In any

convolution, of which auto-covariance is a specialized form, the width of the resulting function on the axis is equal to the sum of the axis widths of the functions being convolved. To allow for this increase in required space, trailing zeros are added to the samples taken. Specifically, if a 128 point transform is to be performed, 64 points will be sampled data points, 64 points will be zeros.

Two more processes are applied to the data array. The first is to determine the mean level and subtract that value from all the data points. Secondly, the Fourier transform requires that the function to be transformed be finitely integratable. The sampled noise function doesn't satisfy that condition. To achieve a finitely integratable function, a "window" is applied to the function to drive the function to zero within the sampled space. The "window" chosen for this experiment is the Bartlett, which superimposes a triangle function upon the sampled data. In the end the sampled data set will look like:

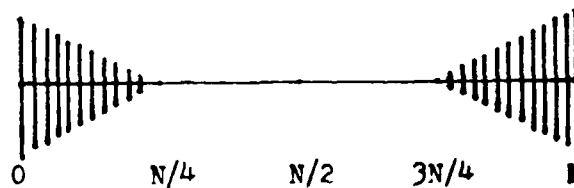


figure 6, Bartlett window applied to Noise data

The transform from the spatial domain to frequency is done using the Tukey-Cooley Fast Fourier Transform algorithm.¹¹ A real and imaginary value results at each data point. The power is determined by taking the square of the modulus of the complex value. The value of the spacing between the data points in frequency is determined by the relation,

$$N \, df \, dx = 1.0, \quad (60)$$

or,

$$df = (N dx)^{-1}.$$

Where N is the number of points in the transform, dx is the sampling interval and df is the data interval in frequency.

Because noise is a random process, the correct application of statistics is critical to insure the noise power spectrum is correctly measured. The standard error in measuring Wiener Spectrum is roughly¹⁸

$$S.E.(%) = (X df)^{-1/2}. \quad (61)$$

Where X is the total scan distance and df is the data interval in frequency. The values chosen will be discussed in the experimental section. The concept of Wiener spectrum will be used in the final measure of image quality, information content.

INFORMATION CONTENT

Information science began with the initial work of C. Shannon¹² and gives considerable insights into the content and capacity of an information system. Primarily, information is a function of the unexpected-ness of an event. Secondly, there is an additivity requirement of information.

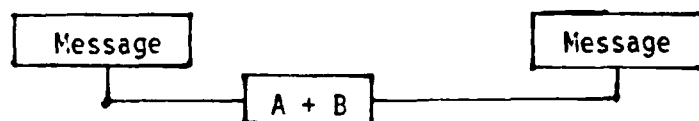


figure 7, Additivity requirement of Information

If the events are independent, so that the probability of both is separable,

$$P(A,B) = P(A) P(B). \quad (62)$$

and the information is additive,

$$I(A,B) = I(A) + I(B). \quad (63)$$

The combination of requirements gives,

$$I(A,B) = f(P(A) P(B)). \quad (64)$$

The only function with this property is the logarithm, therefore,

$$I(A,B) = k \log_b(P(A) + P(B)). \quad (65)$$

For I increasing as $P(A,B)$ decreases, $k=-1$ and viewing all information as ultimately binary, $b=2$. Finally our expression becomes,

$$I(A,B) = -\log_2(P(A) + P(B)). \quad (66)$$

If an image with N_a photo detector elements/unit area is considered, each of which may exist at M number of different levels. Further, all levels are equally probable and adjacent detectors are independent. Then the information capacity in the image will be,

$$I = -\log_2(P(\text{given array of pixel values})), \quad (67)$$

$$I = -\log_2(M^{-N_a}),$$

$$= + N_a \log_2(M), \quad (68)$$

This is only a theoretical limit of information and in no way is an image quality descriptor.

An image quality descriptor that considers both noise and modulation across the dimension of spatial frequency is information coincident. An expression for information content can be derived by considering a stochastic recording media where,

n_p = # of pixel values possible

S = # of stochastic particles per pixel, ie AgX crystals

p_i = probability of observing a pixel value including the true signal and the underlying stochastic process.

f_i = the probability of an observed value given the true value

If,

POP = probability of an observed picture.

POP = number of ways a sequence of pixel values can occur
without repetition times the probability of the observed
sequence occurring

POP = degrees of freedom in the process

Then,

$$POP = \frac{S! f_1^{Sp1} f_2^{Sp2} \dots f_{np}^{Spnp}}{(Sp1)! (Sp2)! \dots (Spnp)!} \quad (69)$$

This is a multinomial distribution which can be better understood if
the signal is a binary process, ie $np = 2$ (yes or no)

$$POP = \frac{S! f_1^{Sp1} (1 - f_1)^{(S - Sp1)}}{(Sp1)! (S - Sp1)!} \quad (70)$$

The information in the picture is,

$$\begin{aligned} I &= \lim_{S \rightarrow \infty} (S - \infty) (1/S \log_2(POP)) \\ &= \lim_{S \rightarrow \infty} (S - \infty) (1/S \log_2(S!) - \sum_{i=1}^{np} 1/S \log_2(Sp_i) \\ &\quad + \sum_{i=1}^{np} p_i \log_2(f_i)) \quad (71) \end{aligned}$$

Using Stirling's approximation for factorials of large X ,

$$X! = \sqrt{2\pi X} (X/e)^X \quad (72)$$

gives,

$$\begin{aligned} I &= \lim_{S \rightarrow \infty} (S - \infty) [1/S \log_2 \sqrt{2\pi S} + \log_2 S - \log_2 e \\ &\quad - 1/S \log_2 \sqrt{2\pi S} p_i - \sum_{i=1}^{np} p_i (\log_2 Sp_i - \log_2 e) \\ &\quad + \sum_{i=1}^{np} p_i \log_2(f_i)] \quad (73) \end{aligned}$$

Applying the limit and canceling terms yields,

$$I = \sum_{i=1}^{np} p_i \log_2(p_i) + \sum_{i=1}^{np} p_i \log_2(f_i) . \quad (74)$$

Information content can be related to capacity by assuming a perfect recording or $f_i = 1.0$ for all i , the equation reduces to,

$$I = \sum_{i=1}^{np} p_i \log_2(p_i) . \quad (75)$$

And if each state is equally probable,

$$I = np \log_2(2) . \quad (76)$$

which is the same as previously defined with the number of levels, $M = 2$

Information on film can be represented by the summing process shown below:

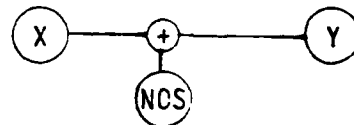


figure 8, Imaging X onto Y with the addition of Noise, NOS

$Y = X + NOS$ where X is the object imaged, and NOS is the total system noise.

$$p_i = P(y)$$

$$f_i = P(Y/X)$$

which is the conditional probability of Y given X . Information becomes,

$$I = \sum_{i=1}^{np} p_i \log_2(p_i) + \sum_{i=1}^{np} p_i \log_2(f_i) \quad (77)$$

In terms of expectation of signal and noise,

$$I = \sum_{i=1}^{np} P(Y) \log_2(1/P(Y)) - \sum_{i=1}^{np} P(Y) \log_2(1/P(Y/X)) \quad (78)$$

$$I = I(Y) - I(Y/X) . \quad (79)$$

The distribution of $P(Y)$ must be found that maximizes the integral,

$$\text{MAX PROB} = \int_{-\infty}^{\infty} P(Y) \log_2(1/P(Y)) dY. \quad (81)$$

This is found when $P(Y)$ is Gaussian or,

$$P(Y) = 1/\sqrt{2\sigma_Y^2} \exp[-(Y - u)^2 / 2\sigma_Y^2]. \quad (82)$$

Applying a Gaussian $P(Y)$ and $P(Y/X)$ to equation 82 at their greatest values gives

$$\begin{aligned} I &= 1/2 \log_2(\sigma_Y^2 / \sigma_{NOS}^2) \quad (83) \\ &= 1/2 \log_2((\sigma_X^2 + \sigma_{NOS}^2) / \sigma_{NOS}^2) \end{aligned}$$

. (84)

The variance, σ^2 , in the signal and noise can be related to its appropriate power spectrum through the Weiner Khintchin theorem which was addressed in the discussion of Weiner spectrum. It can be shown that,

$$\sigma^2 = C(0), \quad (85)$$

further from the central limit theorem:

$$\sigma^2 = C(0) = \int_{-\infty}^{\infty} W(f) df. \quad (86)$$

Information content can now be expressed as,

$$I = 1/2 \int_{-\infty}^{\infty} \log_2[(P_s(f) + P_n(f)) / P_n(f)], \quad (87)$$

where $P_s(f)$ and $P_n(f)$ represent the signal and noise power respectively. Because a photograph is a two dimensional information form, the information in a unit area is represented by,

$$I = 1/2 \iint \log_2[1 + S(v,u)/N(v,u)] dv du. \quad (88)$$

Assuming the image is isotropic and converting to polar coordinates from cartesian with $f^2 = v^2 + u^2$. The equation for information

content becomes,

$$I = \pi \int_0^{f_c} \log_2 [1 + S(f)/N(f)] f \, df, \quad (89)$$

where f_c is the highest critical frequency.

R. Clark Jones¹³ has written about information content in films and his work is based upon the fore-mentioned theory using equation 89. He determined that,

$$S(f) = P(f) \text{ MTF}(f). \quad (90)$$

where $P(f)$ is the power spectrum of the object imaged. In his study he used a set density level in the film. The MTF was calculated from the point spread function of the emulsion.

There are some limitations in Clark's work that must be considered in applying information theory to a photographic system. The first is the limitation of Fourier analysis only to linear systems. While information is conveyed in linear units of exposure, this information is perceived in units of density on the photographic emulsion. Density as a function of exposure is non-linear. However, photographic emulsions can be proven to be quasi-linear over short intervals or a density to energy transformation can be performed. If the density to energy transformation is made, and computations performed on the appropriate energy values, the linear requirements of Fourier analysis are satisfied. However, using energy values diminishes the value of information content as a measure because density is the visually perceived unit. Therefore, density units should be used.

The second problem is information coding on the image. Information content reaches a peak value when the signal is optimally coded which occurs when each grain becomes a unit of information. The grain can

then be represented mathematically as a delta function, whose power spectrum used in equation 90 becomes a constant of unity for all frequency. While theoretically desirable, this information coding would appear as random noise. Any larger image, which would be an aggregation of many grains, would have a power spectrum less than unity for all frequency.

For this study, an edge will be used as the object. The power of an edge in frequency, $Pe(f)$ is proportional to $(f)^{-2}$. To prevent $Pe(f)$ from rising asymptotically to infinity as f approaches zero, $Pe(f)$ will be modified to give,

$$Pe(f) = A / (B + f^2). \quad (91)$$

The value of $B = (0.01fc)^2$ is found from experimental history¹⁴

The auto-covariance of an edge does not exist in a rigorous sense. To employ $Pe(f)$ it must be subjected to some scaling relative to the edge being analyzed to fulfill the condition of the central limit theorem or,

$$\sigma^2 = \int_{-\infty}^{\infty} Pe(f) df. \quad (92)$$

If the edge is considered as an array of points as shown below,

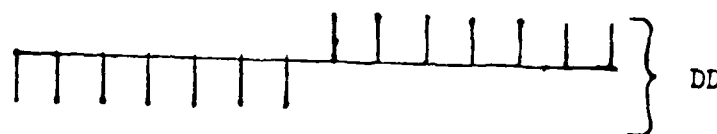


figure 9, Edge as an array of points

Then the variance of that array can be calculated from,

$$\sigma^2 = \lim_{X \rightarrow \infty} 1/2X \int_{-X}^X d(D(x))^2 dx. \quad (93)$$

If DD is the total edge difference, the $d(D(x)) = DD/2$ and $d(D(x))^2 = DD^2/4$. Applying the limit and integrating, the variance of the edge array is now $DD^2/4$. Because of the value of B chosen, if A is set equal to $DD^2/4$ then $Pe(f)$ will be properly scaled.

SUMMARY

The mechanism of CPA has been shown as a photon addition process to achieve a minimum stable latent image state with reduced scene irradiance. Some image quality measures have been defined: contrast, noise, and modulation, and postulated the effect of CPA upon each one. Some laboratory measures relating to these image quality measures have been defined or derived, specifically: DQE, MTF by the second moment approximation, Weiner spectrum, and information content. The experimental section to follow will outline how these techniques will be specifically applied in this experiment.

EXPERIMENTAL

The purpose of this experiment is to evaluate image quality as a function of exposure in a comparison between normally exposed Tri-X Pan emulsion and Tri-X Pan exposed with the benefit of concurrent photon amplification. The hypothesis is that there will exist a distinct exposure region where normal exposure will not yield an image and the CPA treated emulsion will yield a better image in that region. As exposure is increased to a region where normal methods will yield an image, the normal exposure will improve relative to the CPA exposed image and then surpass the CPA image in quality. The diminished contrast and increased noise of CPA exposures should be the prime contributor to this result.

In discussing the conduct of the experiment, there were four distinctive pursuits: 1. Building the apparatus, 2. choosing the film, determining its sensitometry and exposing the samples, 3. performing the microdensitometry, 4. performing the necessary data reduction of the scan data. First, a discussion of building the apparatus.

EXPERIMENTAL APPARATUS

To perform the experiment, a camera equipped with a CPA device, some artwork to image and a mounting system to contain all three principal pieces were needed. The School of Photographics Arts and Sciences at Rochester Institute of Technology provided a suitable Speed Graphic camera body capable of 4 x 5 inch film format and a Fuji 150mm f/5.6 lens.

The CPA circuit and lights were designed and fabricated as shown in figures 10 and 11 respectively. The positioning of the light emitting diodes (LED) was critical to evenly illuminate the film. The lights were placed at the corners of a 3 3/8 inch square and elevated above the film plane so that the irradiance in the corner was equal to the irradiance in the center of the square. The equations for the irradiance at points A and B and the drawings below define the necessary light equilibrium,

$$A = 4 \cos^3(\text{atan}(2.3865/X)), \quad (94)$$

$$B = 1 + 2 \cos^3(\text{atan}(3.375/X)) + \cos^3(\text{atan}(4.773/X)) \quad (95)$$

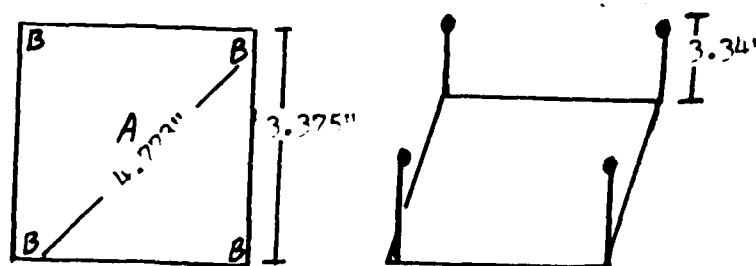


figure 12, Positioning of Light Emitting Diodes

The equations were derived with the assumption that the light emitting diodes would act as a point source. To achieve the desired radiometric balance, A was set equal to B and the equation solved for X. The result obtained was 3.3418 inches. The lights were adjusted to that height. In film tests, this was not perfect because the LED's didn't behave as a point source. However, after some adjustment, there was a central area, about 2" in diameter, (figure 11) where there was no significant density difference. All measurement work was done in that central area.

CPA CIRCUIT SCHEMATIC

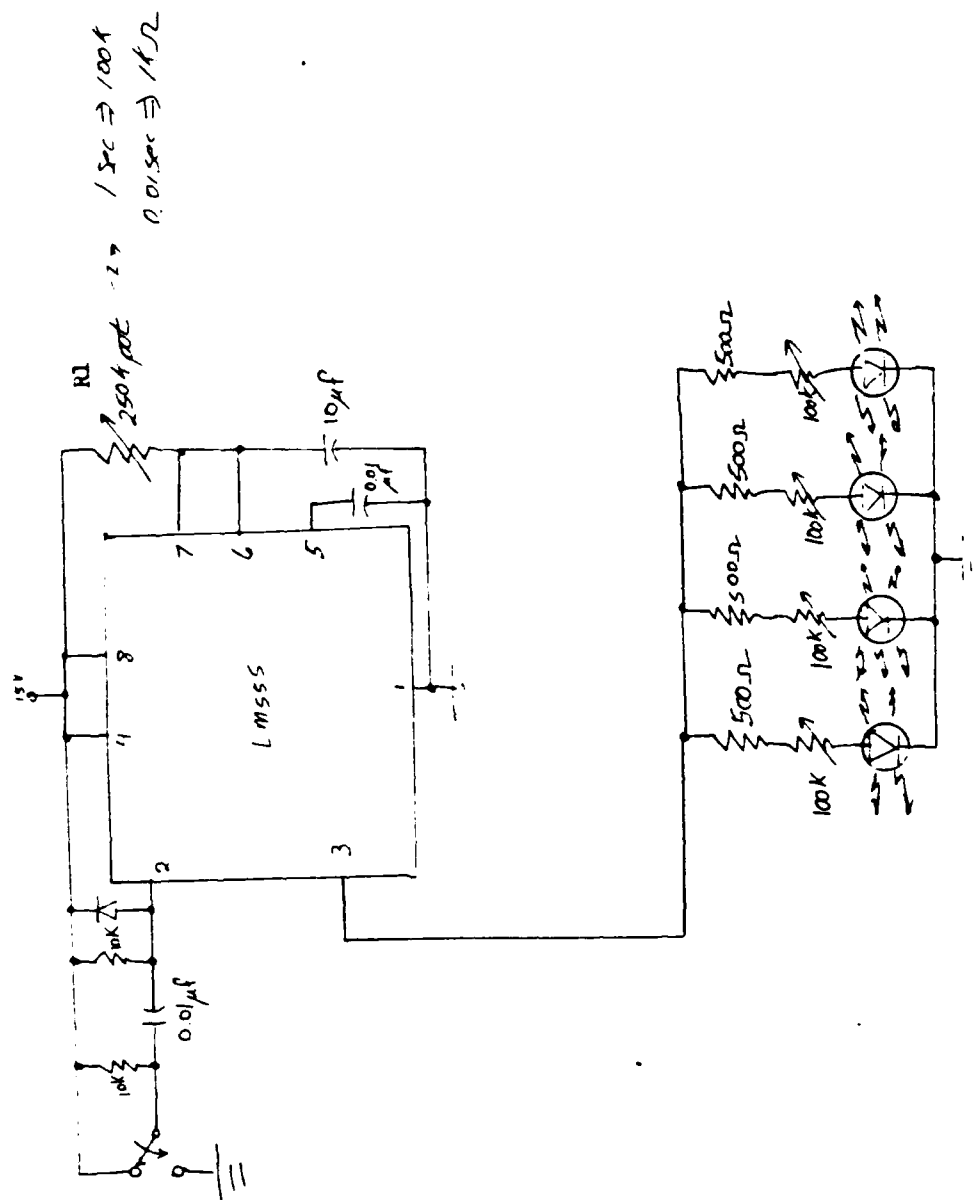
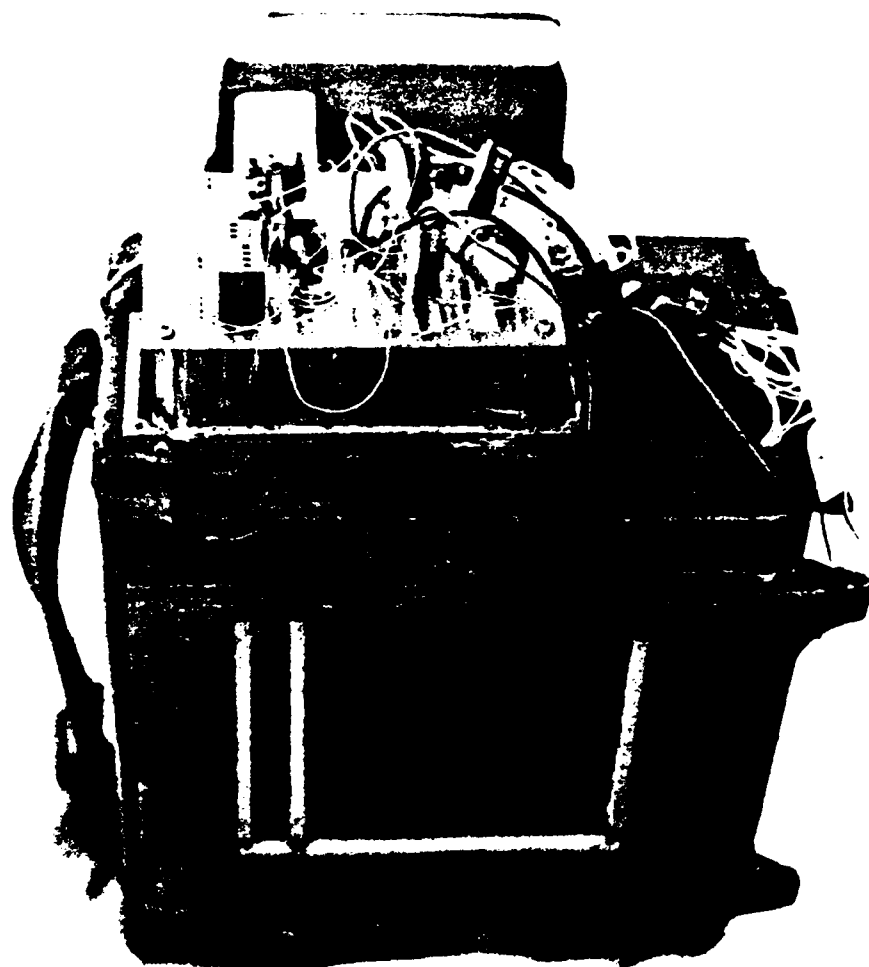


figure 10

figure 11



SPEED GRAPHIC CAMERA
WITH CPA CIRCUIT

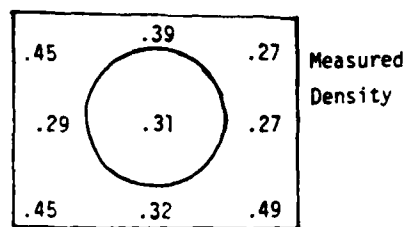


figure 13, CPA irradiance pattern

The lighting was accomplished with a OSRAM 8022 bulb operated at 10 volts 3.7 amps. Power was stabilized with a Thorensen AC2000 power supply with current flow monitored with a Weston ammeter. The light source was used in two ways: First, to trans-illuminate a radial step tablet used to establish the film sensitometry. Secondly, it was configured to give reflected light to the edge art work as shown in figure 5. Irradiance was measured in lux at the film plane using an E.G. & G. radiometer. Placement of the radiometer head was standardized with wooded jig that fit in place of the film holder in the camera back. Using the integrating function of the radiometer, the shutter was calibrated at 1/15, 1/30, 1/60, 1/125, 1/250, and 1/500th of a second. Using film and the E.G. & G. as radiometers, this lighting system was found to be extremely stable and predictable.

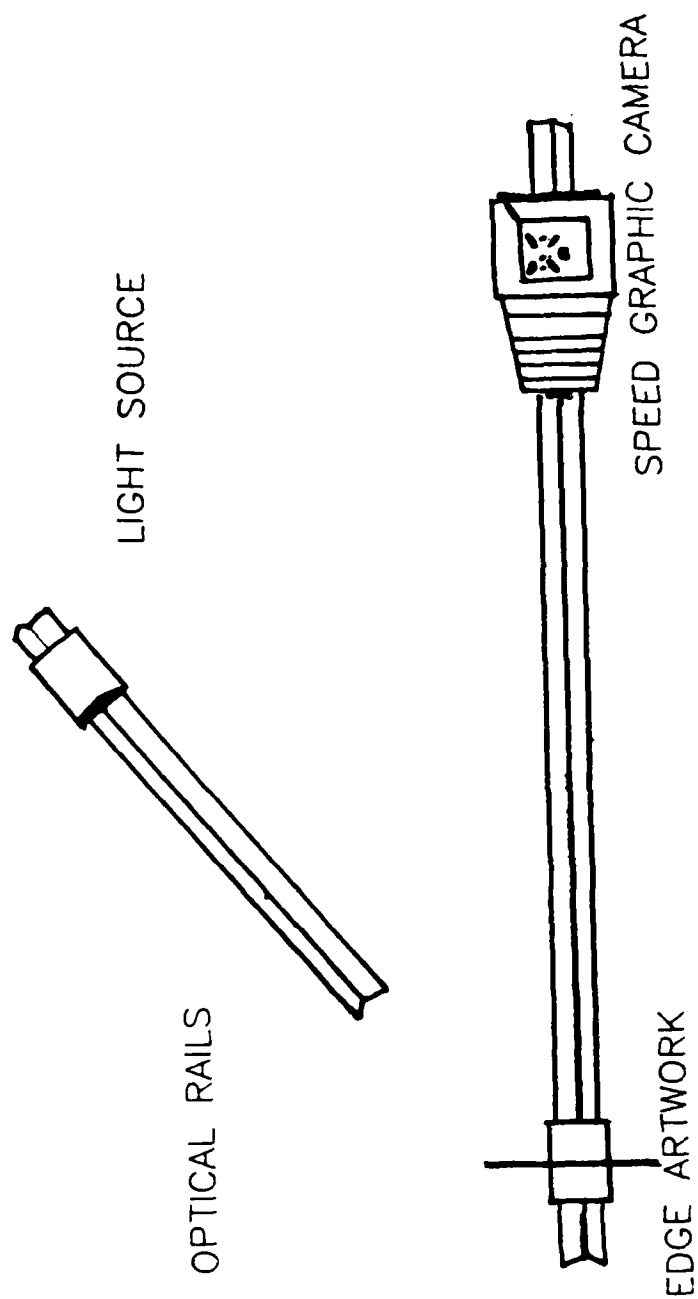
The next requirement was something to image. A standard Kodak radial step tablet was used to determine the sensitometry. The radial step tablet was necessary because of irradiance fall-off from the center of the film plane to the edges. Density was measured at a consistent distance from the center of the pie shaped density pattern.

An edge was necessary to measure MTF. The artwork was made by laying a razor blade across a piece of Kodak 2415 film and exposing. The film was then placed emulsion side facing a Kodak 90% reflection

figure 14

APPARATUS LAYOUT

NOT TO SCALE



card. The purpose of this arrangement was to give even illumination across the light side of the edge to allow ample room to make the Wiener spectrum measurements.

The mounting geometry was shown in figure 14. The optical conjugate relation was set at a magnification of $1/2$. All devices were mounted upon available optical bench hardware attached to the research darkroom counter with tape. An alignment jig was made for the Speed Graphic to insure optical alignment was not disturbed during camera operation.

FILM, SENSITOMETRY, AND EXPOSURE

Tri-X Pan emulsion in a 120 format, emulsion number 5063 819, was chosen as the test film for two reasons: First, this film has figured prominently in former CPA studies. Second, in film, MTF is a function of film speed. The higher the film speed, the poorer the film MTF. The MTF of the film was considered in the belief that the poorer the MTF, the more likely the MTF would be degraded by the CPA effect. Tri-X had the highest film speed, therefore the poorest MTF, of the readily available emulsions. A number of manual development processes were tried and rejected. It was found that a Versamat machine processor gave very good consistency within a batch, ie the variation in density at a set exposure level was less than $\pm .02$ density. The film was processed as a batch with leading and trailing sensitometric strips at 76° , 2.5 feet per minute transport using Versamat 641 chemistry.

The exposure level of the CPA circuit had to be set. The recommended exposure was one that produced a base + fog density 0.10 density units above a normally exposed emulsion. Exposure time in the

CPA device is controlled by resistor R1, which was a decade resistance box. Exposure at various resistance levels and density achieved linearly regressed against resistance. From this analysis, a resistance level was chosen with the final resulting CPA base + fog density of 0.11 above the normal base + fog level.

The final sensitometric curves are shown in the results section. Based upon that information, the experiment would use three exposures exposed with both normal and CPA at -2.07, -1.82, -1.57, -1.46, -1.24, and -.70 log exposure. This was intended to emphasize the low exposure region. Three additional exposures were to made using CPA only at -2.30 log exposure because no normally exposed image was expected. In actually taking the edge images, two exposures were diverted from -0.70 to take one exposure each with normal and CPA at -0.93 log exposure.

The lens was MTF tested at f/5.6 and f/11 at the infinite/focal length conjugates. Based upon those results, the best MTF of the lens appeared to be half way between the two test conditions, or f/8. In taking the edge images the log exposure was determined and an approximate exposure time selected. A 90% reflection card similar to the card used in the edge artwork was placed in the object plane to give a uniform reflection. An irradiance value was calculated and corrected for transmission losses within the film on the artwork. Then the light was moved along its rail until the desired irradiance was measured in the film plane. The radiometer was carefully removed, the film back installed, and three exposures each with and without CPA were made of the edge artwork. The process was repeated until the series was complete. Finally the irradiance was measured in the image

plane as a function of wavelength using the E.G. & G. radiometer with its monochrometer. This irradiance was converted to photons per cm^2 and integrated from 380 nm to 650 nm. The wavelengths of integration were chosen based on the lower limit of the lamp and the upper limit of the film. Then the film was machine processed as formerly described. Because of the variables involved, the whole process had to be completed without interruption. Numerous runs were made incomplete due to various difficulties. In the end, every event was successfully completed and the desired exposure series gathered.

MICRODENSITOMETRY

The microdensitometry was performed on a Perkin-Elmer PDS system tied to a PDP-11 for data processing. Normal MTF measurement of an edge is performed with the assumption of a "global" edge, meaning an edge that is effectively infinite in length with resolution becoming a one dimensional problem. Within imagery, a "global" edge is often inappropriate as the object to be resolved will be two dimensional with comparable sizes in the orthogonal directions. To evaluate the effect of noise on measuring these non-global edges, a 10 x 25 micron slit was chosen. Forty exactly adjacent scans of the edge were made with a sampling interval of 3 micron for 1024 points. Considering the convolution of the slit with the data, the single slit gave a two dimensional frequency domain of 40 x 100 cycles per millimeter (cpm). The positioning accuracy of the microdensitometer used was such that the scans could be averaged to give a variable frequency domain. If two scans were averaged, the frequency domain available was 20 x 100 cpm

and if four scans were averaged, the domain was 10×100 cpm. Finally if all 40 scans were averaged, the domain was 1×100 cpm. The averages mentioned were those made in the processing. The 10, 20, and 40 cpm frequency domain roughly corresponds to the extremes and center of the human visual response measured at the cornea. The average of the forty scans was the "global" edge and was used to compute the MTF for the information content computations.

Weiner spectrum data samples were taken with a 124×6 micron slit at a sampling interval of 3 micron. Data was taken in blocks of 64 so that zeros could be added to fill a 128 point transform. 105 blocks of data were taken to give a total of 6670 data points per exposure. This gave an X distance of data equal to 20.01 mm which gave a standard error of 13%.

SOFTWARE

Computer software was written in Fortran 77 to perform the necessary computations. Three principal programs were operated from a command file. The first of these performed a forty scan average of the edge data. 300 points at each end of the scan were averaged to determine D_{max} and D_{min} . The scan was then evaluated to determine the exact extent of the edge by value comparisons between data points and the D_{max} and D_{min} values. The array number for the beginning and end of the edge as well and the edge midpoint and D_{max} and D_{min} were passed via a data file to the second program.

The second program took the D_{max} , D_{min} , and edge coordinates and made MTF computations using the second moment approximation for

singular scans and averages of two, four, and forty scans. The maximum number of M_2 values that could be calculated from the available data were 40, 20, 10, and 1 respectively. The edges were always scanned from light to dark. If a negative value of M_2 was computed, this was considered a bad edge and that value was rejected from the statistical computations of mean and standard deviation. The number and values of good M_2 's and their summary statistics for all considerations were output to printer. The forty scan averaged M_2 and the edge density difference were output to screen and used in the third program.

The third program read the noise data in blocks of 64 and computed the density variance and the mean value of the 64 data points. The mean value was subtracted from each data point and the array doubled in size with the addition of 64 trailing zeros. The Bartlett window was applied and the 128 point array Fourier transformed. The power of the noise was achieved by taking the square of the modulus of the transformed output. This process was repeated 105 times with ensemble averaging of the resulting Wiener spectrum. To determine if the frequency content of the Wiener spectrum shifted with exposure, the first moment of the array was computed from 0 to f_{max} . Finally, the program prompted for contrast, exposure in photons per cm^2 , averaged M_2 , edge density difference and sample identification information. The program computed DQE and information content and output Wiener Spectrum and all values read during the prompting and computed by the program.

All software was evaluated with known input data to insure computational accuracy. The programs are attached to the thesis as attachments 1, 2, and 3.

RESULTS

The results given in this section are presented in the order they were developed in the experiment an/or derived in the theoretical section. For ease, all the figures referenced in the results section are grouped together at the end of the thesis. The data conveniently groups into three major blocks leading to the principal measures of this study: 1.Sensitometry, contrast, density variance, and DQE 2.MTF 3. Edge step difference and information content. In many cases the standard deviation of the data was an order of magnitude less than the mean. In those cases, only the mean value at an exposure level is presented. When appropriate, regression analysis is performed and plotted with the data.

Many of the results followed the hypothesis very closely. When it is appropriate, this observation will be made with the data. The exposure point where the preferential method changes from CPA to normal will also be addressed. A detailed discussion of the results that do not directly follow the hypothesis and an overall summary of the data and the conclusions to drawn will be presented in the following section. First, the results leading to DQE will be presented.

FILM SENSITOMETRY AND DQE

Figure 15 shows the sensitometry for the film process. There is approximately 1 stop or 0.30 log exposure difference between the processes, the speed points are annotated on the figure. The film speed difference is lower than previously published 6 stop advantage for CPA. The difference lies in the present use of a quantitative measure of the

speed point given by the exposure level that gives 0.10 density above base + fog. A subjective measure was used to evaluate the film speed difference in the referenced article.

The sensitometric curves were fit by least squares to a quartic equation. The first derivative of the two equations were taken with the results plotted in figure 16. This shows the available contrast at each exposure level and is the beginning of a result that continues through much of the data. CPA possesses a distinctive exposure domain where it will produce a better image. As exposure increases, the normally exposed image improves and then surpasses the CPA image. For contrast, the cross-over point, or log exposure level where the preferential exposure changes from CPA to normal is -1.92

Figure 17 is a plot of density variance vs log exposure. This measure of noise in the signal shows CPA to have a significant disadvantage until very high exposure. Figure 18 shows DQE vs log exposure. The DQE relation shown in equation 45 is very sensitive to change in contrast or gamma. The advantage normal exposure possesses in gamma and $d(\overline{D})^2$, where normal exposure will produce an image, is immediately apparent. The dashed extension of the normal exposure DQE line is extrapolated data based upon the exposure level where gamma would reach zero. CPA holds an advantage over normal exposure only below -2.07 log exposure.

MODULATION TRANSFER FUNCTION

Modulation transfer function was the most intensively studied aspect of this experiment. Two distinct data sets are presented:

first, MTF calculated with a global edge. Second, MTF calculated with increasing orthogonal frequency domain and greater noise. First the MTF data calculated with the global edge.

Figures 19 and 20 present the second moment calculated for normal and CPA exposures respectively. A smaller value of M_2 means a better MTF. The data was fit to a cubic equation by the least squares method with the regression equations shown below, $1e = \log \text{ exposure}$,

Normal,

$$M_2 = 4.9299 + 10.22 \, 1e + 9.90 \, 1e^2 + 2.79 \, 1e^3$$

$$R^2 = .5749$$

CPA,

$$M_2 = -8.0702 - 22.96 \, 1e - 14.94 \, 1e^2 - 2.96 \, 1e^3$$

$$R^2 = .3169$$

Figure 21 shows the regression lines, without the data points, together on the same chart. A complete discussion of the factors impacting the measurement of MTF will be presented in the discussion section to follow. Recalling that lower M_2 means a better MTF, CPA does not possess a clear advantage in the low exposure domain. Normal exposure is clearly preferential in the high exposure domain beginning at $-1.70 \log \text{ exposure}$.

Figure 22 shows M_2 v. $\log \text{ exposure}$ with various slit lengths for the normal process. The dimensions of the orthogonal frequency domains were discussed in the experimental section. As the ratio of the orthogonal frequency domain increases, there appears to be less exposure dependence in the value of M_2 . Alternatively stated, M_2 seems to improve with exposure in the least averaged or most noisy

scans. As the averaging decreases the noise, M_2 doesn't seem to improve with exposure as markedly. Figure 23 shows the standard deviation in the M_2 measurements in figure 22. Figure 24 shows the ratio of "good edges" that were used in computing the data for figure 22. Figures 23 and 24, show in general, the confidence to perceive an edge improves with increasing exposure and diminished orthogonal frequency domain.

Figures 25 to 27 show the equivalent results for the CPA process to figures 22 to 24 for the normal process. CPA results are generally similar to those of normal exposure with an exception. The ratio of good edges does not follow the same pattern as normal exposure. For short slit lengths, the ratio of good edges reaches a peak less than 1.00 and falls off slightly with increasing exposure.

INFORMATION CONTENT

Figure 28 shows the edge difference between the macro maximum and minimum density across the edges. This value is used to compute the power spectrum of the edge as shown in the theory introduction. The domains are clear where CPA and normal exposure are advantageous with the cross-over occurring at $-1.46 \log$ exposure. Recall the subjective six stops difference between CPA and normal exposure vice the quantitative one stop difference used in this experiment. The subjective measure may be more appropriate considering the shallow slope of the CPA contrast and edge difference curves. The CPA process may give a acceptable image well below a quantitatively determined speed point making a six stop difference very reasonable. This effect

was not considered in establishing the sample collection scheme.

Figures 29 and 30 show the information content vs log exposure for normal and CPA exposure respectively. The information content was linearly regressed against log exposure with the equation values presented below,

Normal

$$I.C. = 387.91 + 151.98 \log e$$

$$R^2 = .7949$$

CPA

$$I.C. = 236.28 + 69.78 \log e$$

$$R^2 = .6319$$

In the comparison of these two charts there are two distinctive domains wherein each technique has an advantage. The cross-over point for this measure is $-1.84 \log e$.

Conspicuous by its absence is data concerning the Wiener spectrum. The first moment of the Wiener spectrum was computed and found not to change as a function of exposure. From the central limit theorem the integration of the Wiener spectrum over all frequency is equal to the variance. Further, from figure 17 the density variance increases monotonically with exposure at a rate dependent on whether normal or CPA exposure is used. For completeness, figure 31 shows a typical Wiener spectrum. The impact of the Wiener spectrum on the information content equation is one of an increasing denominator factor with increasing exposure. The power spectrum of the edge is generally increasing as a numerator factor with increased exposure. The last numerator factor, MTF in some domains of exposure is also generally

increasing with exposure. The result is a competitive rate problem. Judging from the information content results the numerator factors, edge power spectrum and MTF, increase faster than the noise as a function of exposure.

A more complete discussion of these results and conclusions to be drawn from them will follow in the next section.

DISCUSSION

INTRODUCTION

This discussion section will begin with a re-statement of the hypothesis. There is a distinct region in which CPA will provide an image, and normal exposure will not. Within that region, CPA by default provides the better image. There exists a region in which both CPA and normal exposure technique will provide an image. As the exposure level increases in this region, the quality of the normally exposed image will improve to equal and then finally surpass the quality of the CPA generated image. There are some results that directly support that hypothesis. Specifically these are the comparative values of contrast, DQE, edge step difference, and information content as a function of exposure. There are two data sets within the results section that are not immediately supportive of this hypothesis. These are density variance and MTF as a function of exposure. For brevity, this section will only address the data non-compliant with the hypothesis. Secondly, the nature of the cross-over point will be discussed. This is the exposure level at which the preferential exposure means changes from CPA to normal. First, a discussion of density variance.

DENSITY VARIANCE

As previously stated density variance is a measure of noise. This result is not in strict compliance with the hypothesis but is a reasonable result because CPA has added noise which will never diminish below the base level achieved on the film. Therefore, in reviewing this result, shown in figure 17, the noise level, or variance increases with

increasing exposure at a rate dependent upon the exposure technique used. The results also show the noise level in the CPA emulsion is always higher than the normally exposed image, but the difference decreases with increasing exposure. This is a relatively minor deviation from the hypothesis stated and does give interesting information in regard to the additive noise given by the CPA effect.

MTF

MTF does not follow the hypothesis directly as stated. There are a number of reasons for this and include both errors in measurement and real changes in the MTF. Artificial changes in MTF result from measurement errors, primarily from noise. Noise effect is inseparable from the measurement but one can postulate the effect based upon the condition under which the MTF measurement was made. There are two possible sources of real change of the MTF which will be discussed, the first of these is the change in the perceived point spread function as a function of exposure, the second is related to adjacency effect.

Noise has a bidirectional effect dependent upon the power of noise relative to the power of the signal and the variance of the noise across the edge. This effect can either help or hinder the MTF measurement. Alternatively, noise will either give an inflated measure or deflated measure of MTF. In the case of an inflated measure the measure will be considered inaccurate and not representative of the true MTF but rather an artifact of measurement. In the case where noise would hinder the MTF measure, this a realistic measure of the operative MTF because that noise effect would be a factor in any viewing of the image.

Noise can be a help or enhance the measure of MTF when two specific conditions are met. One, the edge being scanned is relatively low contrast and the noise is statistically stationary across that edge. Second, when the noise power is significantly less than the power of the edge. Under these conditions the noise will add a random phase factor with the average result being an improvement in the measured MTF¹⁹.

The effective noise can hinder or can reduce the measured MTF, when two conditions mentioned above are not present. Either the power of the noise is greater than the power of the edge or the noise is not statistically stationary across the edge. If either of these conditions are present, noise will hinder high frequency signal, thereby reducing MTF.

As stated in the introductory paragraph of this discussion of MTF, the effective noise is either a help or hindrance and becomes a measurement artifact in evaluating MTF. There are two distinct factors which change as a function of exposure and do result in a distinctive change in the MTF. The first of these is the change in the point spread function as a function of exposure. In general, the line spread function of an entire imaging system on an emulsion will take the form shown below:



figure 32, Typical Line Spread Function.

This form will vary with optical aberrations involved and chemical effects induced in the film. Assuming radial symmetry, the key point is the shape of the point spread function narrows as it approaches the peak and has a distinctive slope function as it approaches its null. Within a photographic emulsion there is a measurable domain given by the density above base + fog. The shape of the point spread function in a rigorous sense will not change, however, the measurable domain of that point spread function will change as a function of exposure.

An analogy to a volcano creating an island is very appropriate. The island does not change shape in an absolute sense. However, as the volcano generates more island form, so that the island emerges above the surface of the water, the shape of the volcano becomes broader to those viewing from above the water. In an analogy to a photographic system, there is a base + fog level on the film which equates to the water in the example. As increased exposure elevates the point spread function of the imaging system above this base + fog level, the visible domain will tend to broaden until the first null is reached. After the first null is above base + fog, there will not be any relative increase in the width. The volcano analogy loses some of its value because the width of the volcano is not subject to any finite limitations. The imaging system point spread function does have a limiting size based upon diffraction and the aberrations of the system. However one may generalize that MTF will diminish slightly with increasing exposure due to the visible or measurable domain of the point spread function.

There is an ancillary effect within photographic emulsions called adjacency effect.²⁰ The adjacency effect is created by chemical

anisotropy which results from the unique nature of hydroquinone based developing solutions. Where the edge occurs there will be a relative area of high density requiring exhaustive chemical efforts and low density requiring relatively little chemical effort. The nature of hydroquinone based developers is such that where there is increased developer activity, the exhausted developer will locally change the pH of the development solution resulting in increased developer activity. The apparent effect upon the emulsion is that the dark get darker, lights get lighter at the boundary. Agitation will reduce this effect. Machine agitation in the Versamat should normally be adequate, however more vigorous methods would have reduced the adjacency effect more. The effect is shown in the diagram below:



figure 33, Example of adjacency effect

The net result is that this will tend to improve MTF with increased adjacency effect with increases with increasing exposure.

An attempt to correlated these effects to the results is very complex, but some postulation can be made. In viewing results figure 19, at low exposure the noise has relatively low power and is statistically stationary across the edge. The result is an improvement in the measure of MTF due to this random phase factor given by the noise under these conditions. Secondly, at this exposure there is a small apparent point spread function, again resulting in improved MTF.

As the exposure increases, three factors are occurring, one the noise loses its stationary quality. The noise power also becomes greater. The point spread measurable domain expands and finally, the adjacency effect given by the developer improves. Reviewing the results we can see a marked rise in the M_2 , followed by a rather slow decline in M_2 or improvement in MTF. In the region where MTF is gradually improving, the predominant effect seems to be the adjacency effect.

In reference to results figure 22, one can see the effect of noise, adjacency effect, and point spread function visible domain in measurements where the power of the noise is significantly greater. The inclusion of this noise destroys the available high frequency signal resulting in a diminished MTF measured. As the noise is reduced through greater averaging and reduced orthogonal frequency domain, the measured MTF values approach those measured with a global edge. Therefore, in the presence of noise the ability to detect a two dimensional object with comparable orthogonal measurements significantly improves with increasing exposure. As the ratio of the object dimensions increase, the exposure dependence decreases. this result is also shown in results figure 24, the ratio of good edges. The ratio improves with increased averaging and increased exposure. Further, the relative slopes of the lines diminish with increased averaging.

Many similar arguments apply to the CPA exposed images both with the global edge and the increased noise measurements. Because there is a unique domain in which only CPA will give an image, any MTF measured will be better than the normally exposed image measured MTF. The M_2 increases to a peak level and then begins a rapid decline to converge

upon the normally exposed value. The reason for the shift in the peak location towards higher vs lower exposure is not clear. In reference to measurements made with increased noise and orthogonal frequency space, many of the trends seen in the normally exposed images are apparent. There is an exception noted in the results section concerning the ratio of good edges not converging to one. System noise in the measured values coupled with a reduced adjacency effect in the CPA images are possible explanations.

Considerable emphasis has been given to minute differences in the measured M_2 values and attempts made to derive conclusions on them in relation to exposure. Much of this may be unfair in light of a statistical analysis of the data. In both normal and CPA cubic regressions of the global edge data, the R^2 is relatively low, especially for CPA. Linear regressions for both data sets included a slope of zero within a 90% confidence limit, indicating that there is no exposure dependence. The second moment approximation for MTF is sound, however its ability to accurately depict complex changes in MTF given with the addition of flare may be questionable. Alternatively, a more comprehensive measure of MTF would not as easily lent itself to an analysis relative to exposure. With reference to figure 2, there should be some measurable improvement of MTF with exposure. A possible future work could be some power spectrum analysis of edge data as a function of exposure to more clearly determine this exposure dependence of MTF. To conclude the remarks on MTF, there may be an exposure dependence of MTF that is affected by the variety of factors mentioned. Unfortunately, the data does not support that conclusion with the greatest strength.

CROSS-OVER POINT

There was not a clear agreement within the data on a boundary exposure where the preferential exposure method changed. The cross-overpoint was measurement specific and there was a range in which the measurements experienced their cross-over. For review, they are listed below:

Measurement	Cross-Over Point (log exposure)
Contrast	-1.92
DQE	-2.07
M ₂	-1.70
Edge Difference	-1.42
Information content	-1.84

The mean value of the cross over point was -1.79 log exposure with a standard deviation of 0.246. This average point corresponds approximately to the half speed point or 0.15 log exposure below the normal exposure speed point. Because of the high standard deviation, one would infer a boundary region rather than a point. Further, the use of CPA in an exposure region below the highest boundary point should yield the preferred image. With decreasing exposure, the benefit of CPA relative to normal exposure will be enhanced.

CONCLUSIONS

In summary three distinct conclusions can be drawn from this study which represent the assertion of the initial hypothesis. There are:

1. There is a low exposure domain in which only CPA can give an image. The size of that domain is a function of the means of measure. For a quantitative measure, the size is modest, only one stop in this study. However if a subjective measure is employed, that CPA domain of preference could be larger, as much as six stops.

2. There is a domain where both CPA and normal exposure will produce an image and in this domain, CPA will give a better image than normal exposure. The benefit of CPA diminishes towards the high end of this transition domain.

3. Above the transition domain, normal exposure will yield a better image than the CPA treated image.

BIBLIOGRAPHY

1. Class room instruction from Dr. R. Francis, RIT, July 1982
2. R.P.Czwakiel, E.C. Scott, SPIE 58, 58-5 (1975)
3. T.H. James, Theory of the Photographics Process 4th Ed, MacMillan NY 1977 p105
4. M.R. Cole, RADC Contract F30602-73-C-0071 (1974)
5. Granularity, Kodak Publication F20, Rochester NY (1979)
6. H.E. Spencer, J Phot Sci 24, 34 (1976)
7. W. Brouwer, E.O'Neill, and P.Zavracky, Some Factors limiting Bit Capacity in Electrophotographics Systems, Unpublished Coulter Systems paper.
8. J.C. Dainty, R. Shaw, Imaging Science, Academic Press, San Francisco 1974 p138
9. N.Weiner, The Fourier Integral and Certain of its Applications, Dover Publications inc, New York, 1958
10. W. Brouwer, Matrix Methods in Optical Instrument Design, W.A. Benjamin Inc, 1964 p 275
11. R.Gonzalez, P.Wintz, Digital Image Processing, Addison Wesley Inc, Reading MA, 1977 p 80
12. C.E. Shannon, Mathematical Theory of Communication, University of Illinois Press, Urbana IL (1949)
13. R.C. Jones, J Opt Soc Am 51, 1159 (1961)
14. Personal Conversation with J. Sullivan, May 8 1984, Rochester NY
15. Class room instruction from Dr. E. Granger, RIT, April 1982
16. T.H. James, Theory of the Photographics Process 4th Ed, MacMillan NY 1977 p 538
17. J.C. Dainty, R. Shaw, Imaging Science, Academic Press, San Francisco 1974 p 1-29
18. J.C. Dainty, R. Shaw, Imaging Science, Academic Press, San Francisco 1974 p 296

BIBLIOGRAPHY,cont

19. J.C. Dainty, R. Shaw, Imaging Science, Academic Press, San Francisco 1974 p256

20. T.H. James, Theory of the Photographic Process 4th Ed, MacMillan NY 1977 p405

21. J.C. Dainty, R. Shaw, Imaging Science, Academic Press, San Francisco 1974 p360

figure 15

DENSITY V. LOG EXPOSURE

NORMAL CPA
SPEED POINT ↑

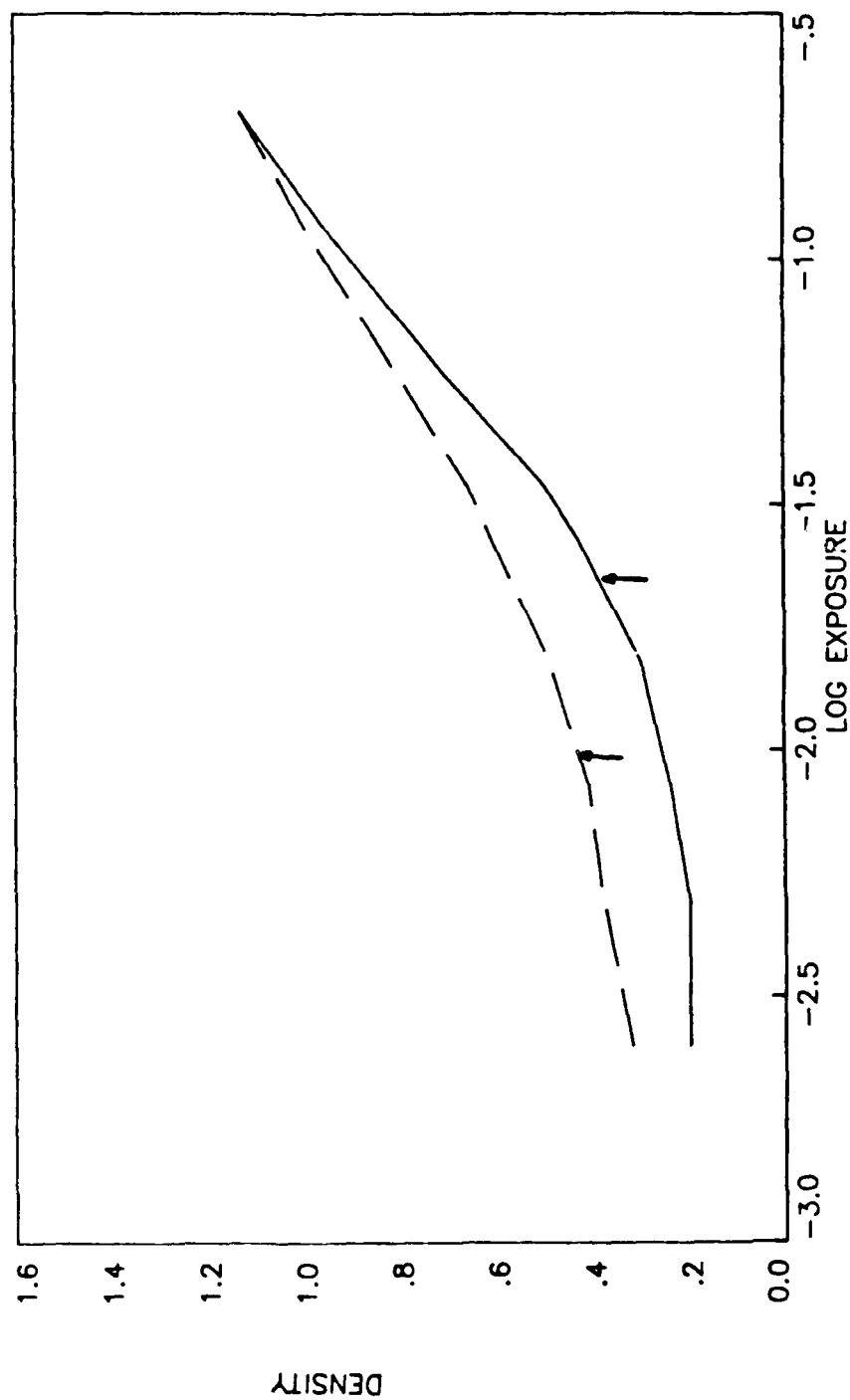


figure 16

CONTRAST V. LOG EXPOSURE

NORMAL CPA

— - - -

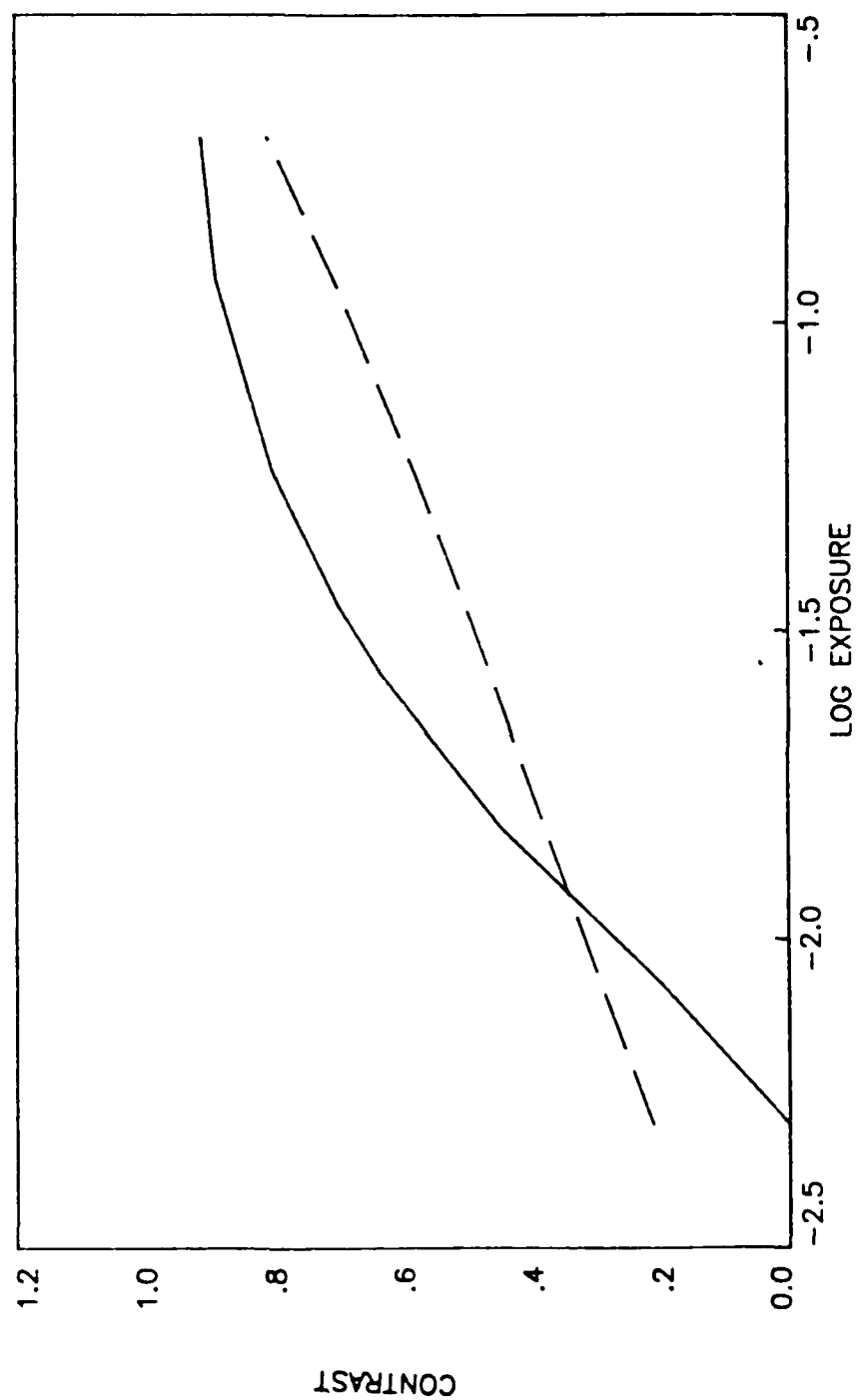
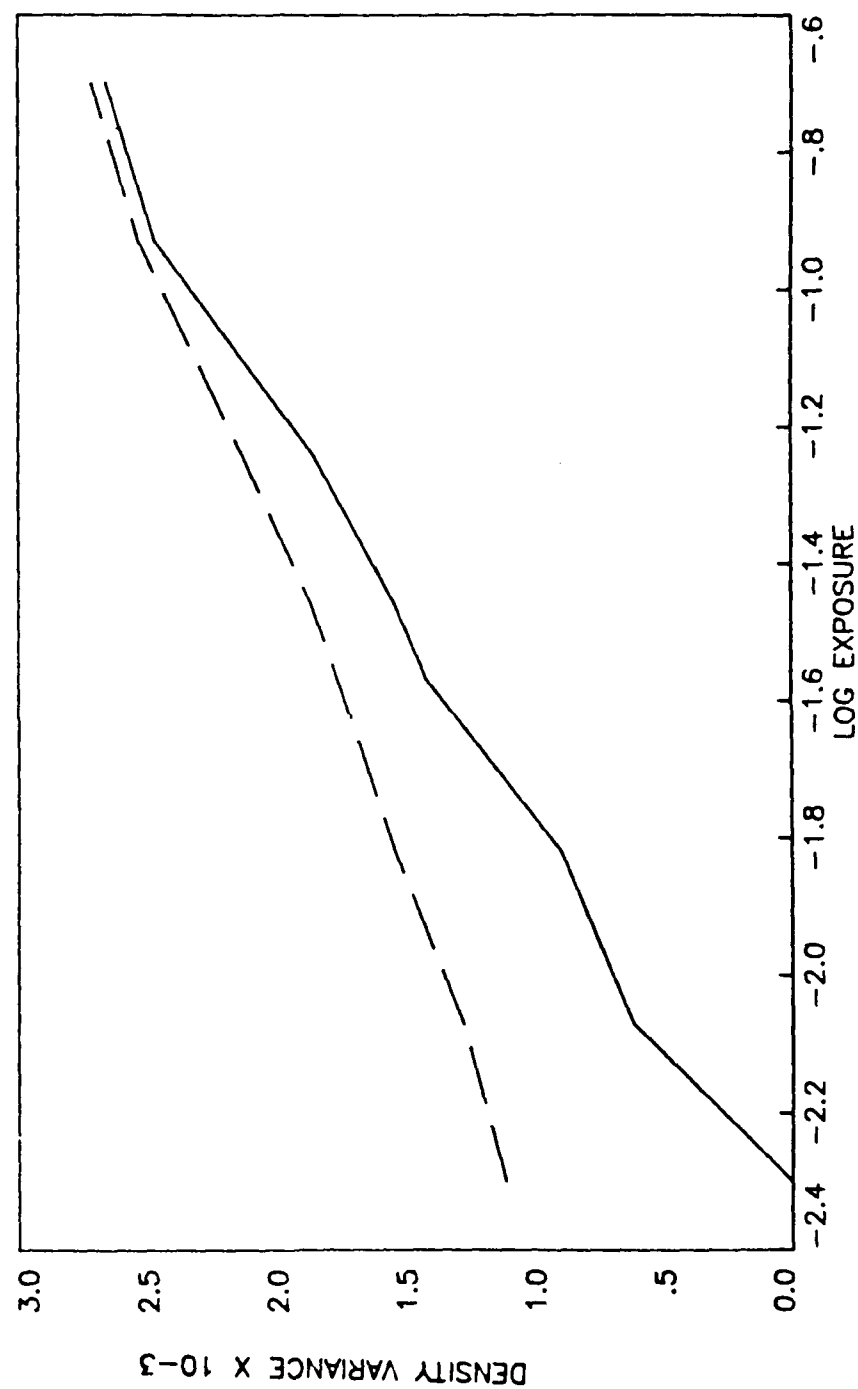


figure 17

DENSITY VARIANCE V. LOG EXPOSURE

NORMAL

CPA



DQE V. LOG EXPOSURE

NORMAL CPA

— — —

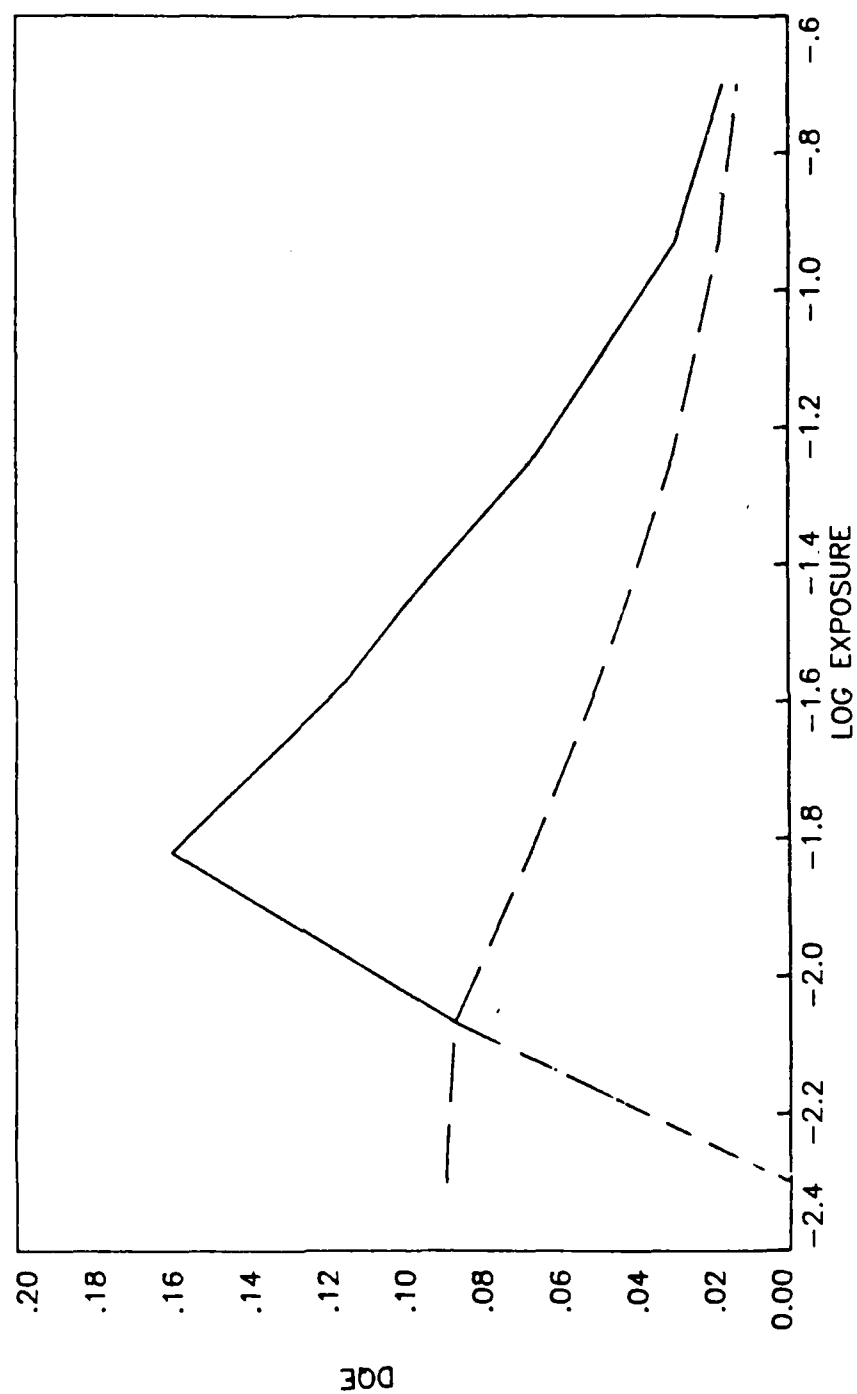


figure 18

figure 19

SECOND MOMENT V. LOG EXPOSURE
NORMAL EXPOSURE

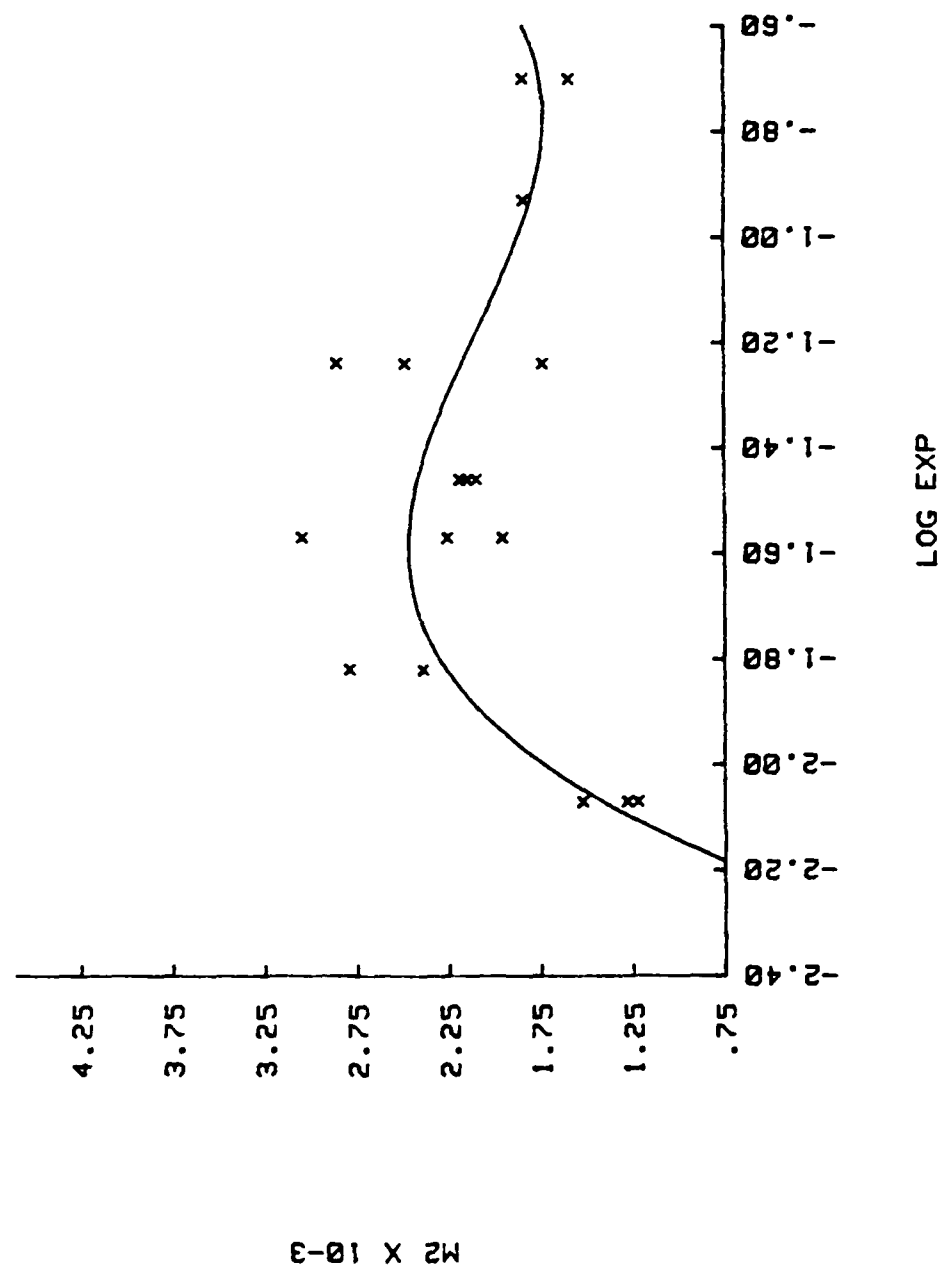
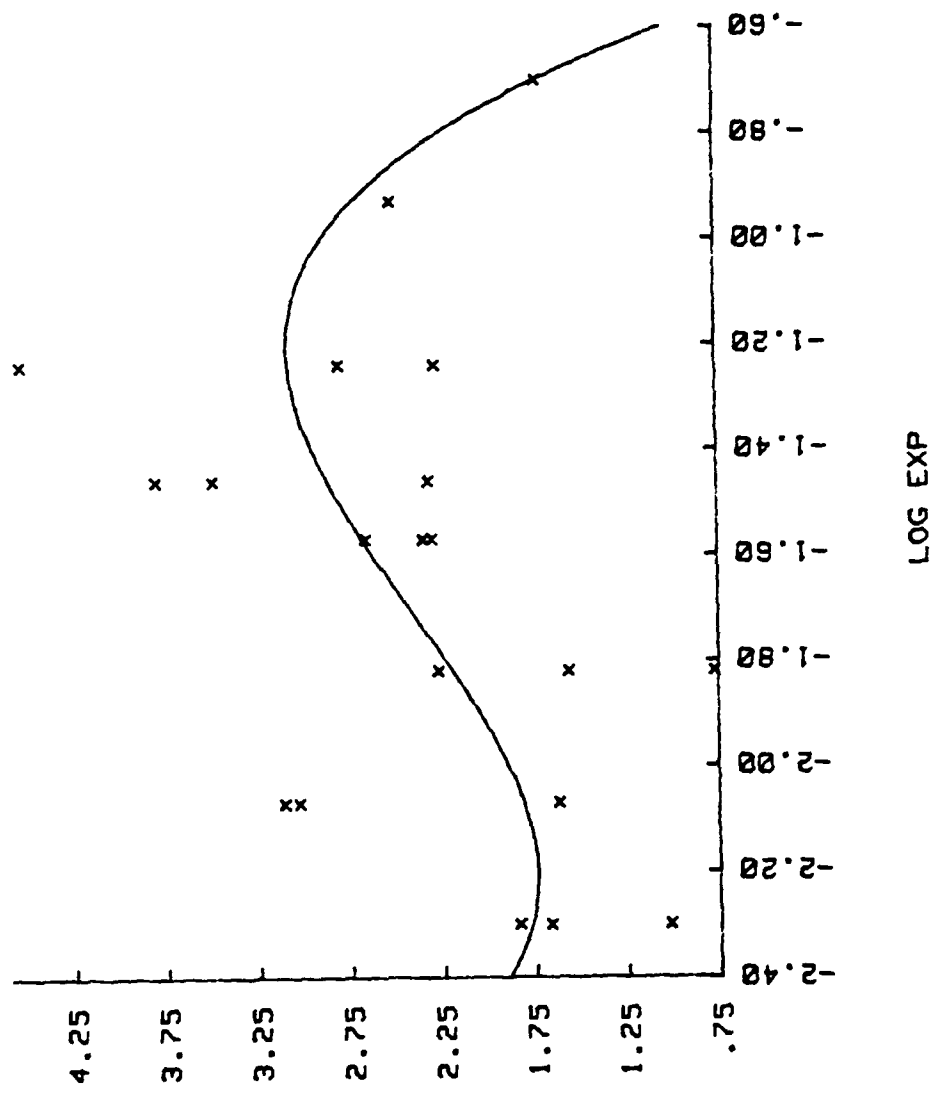


figure 20

SECOND MOMENT V. LOG EXPOSURE
CPA EXPOSURE



M2 X 10-3

figure 21

SECOND MOMENT V. LOG EXPOSURE

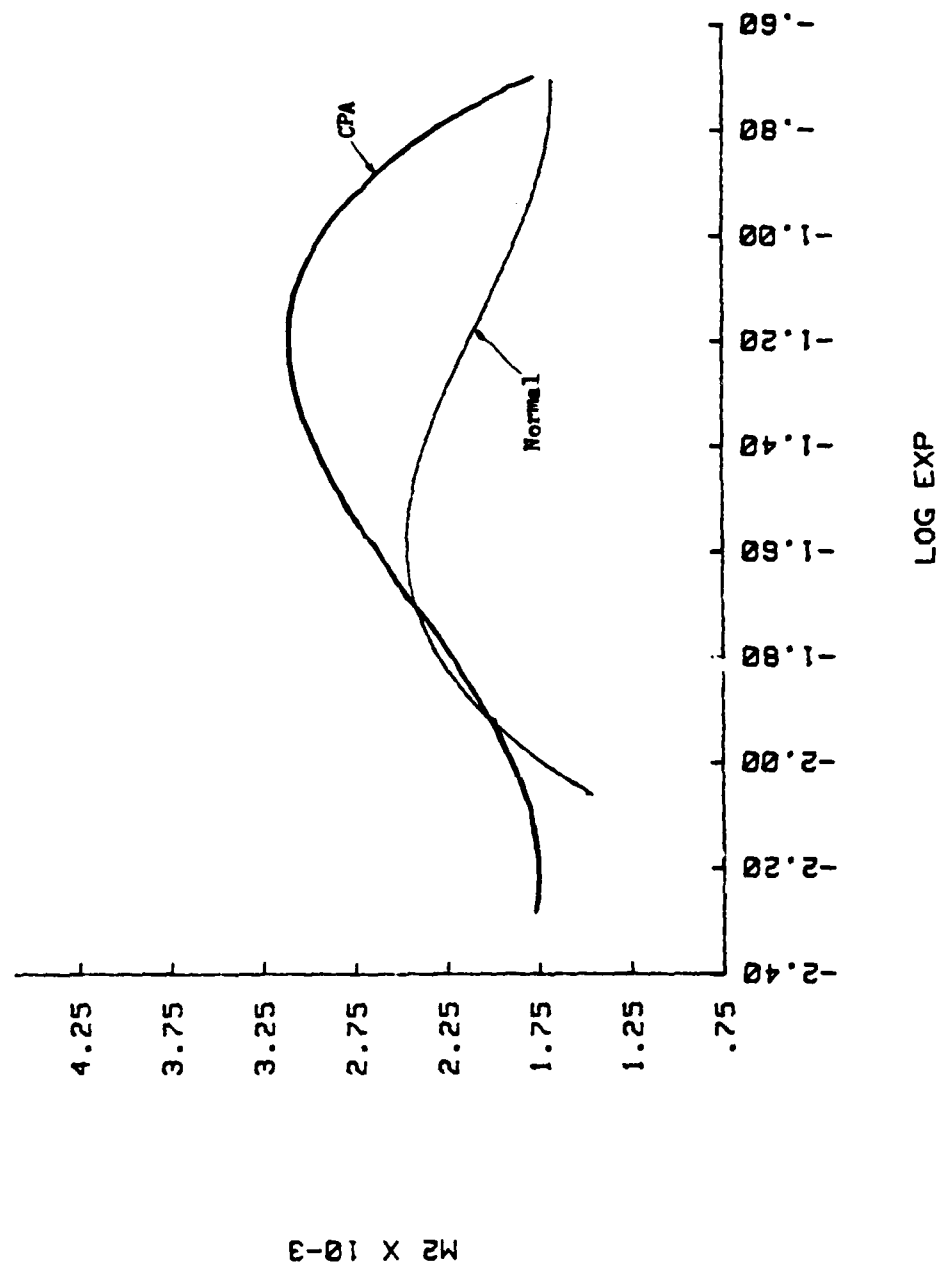


figure 22

SECOND MOMENT V. LOG EXPOSURE

NORMAL EXPOSURES

1 SCAN

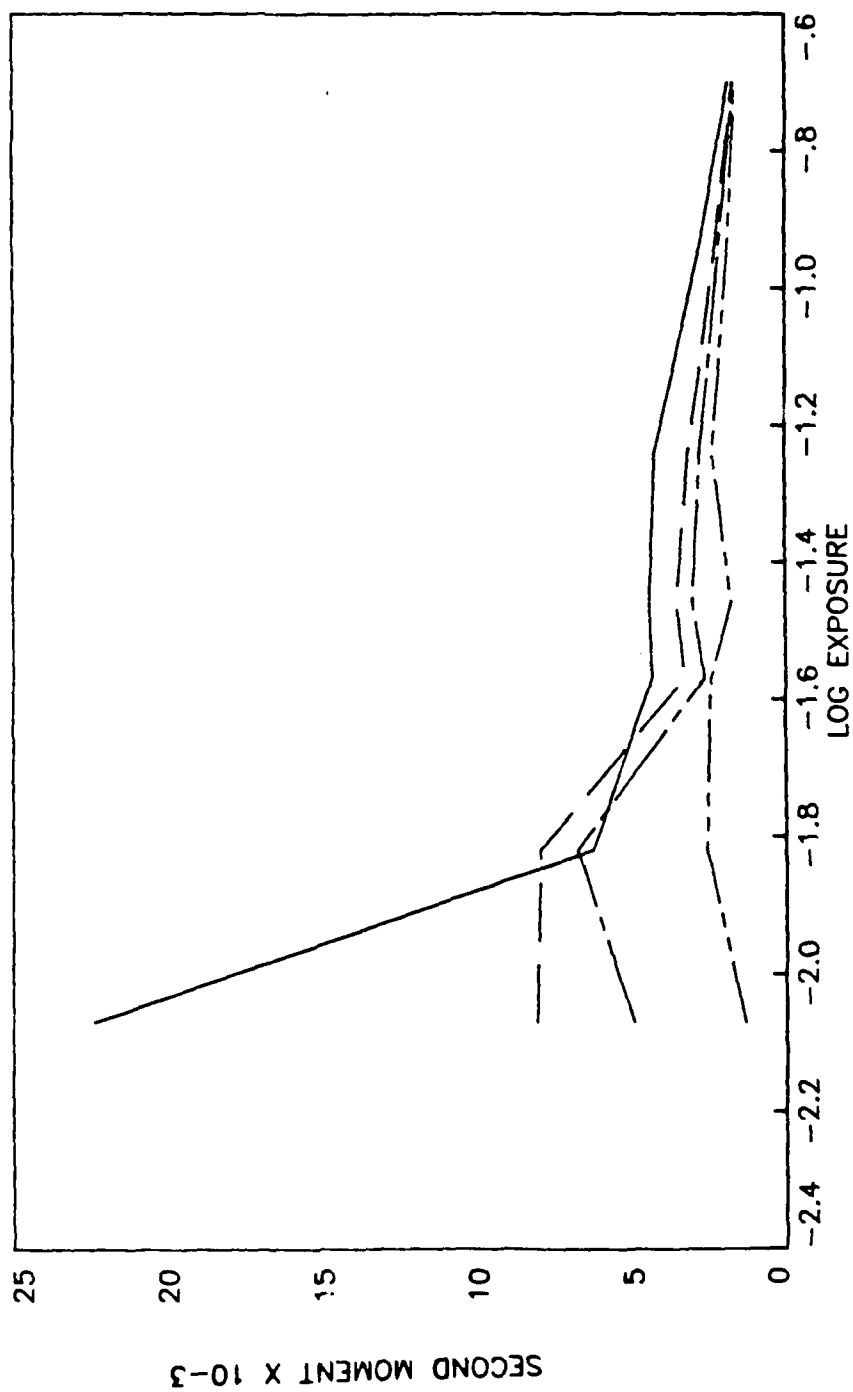
2 SCANS
AVERAGED4 SCANS
AVERAGED40 SCANS
AVERAGED

figure 23

M2 SDEV V. LOG EXPOSURE
NORMAL EXPOSURE

1 SCAN	2 SCANS AVERAGED	4 SCANS AVERAGED
---	---	---

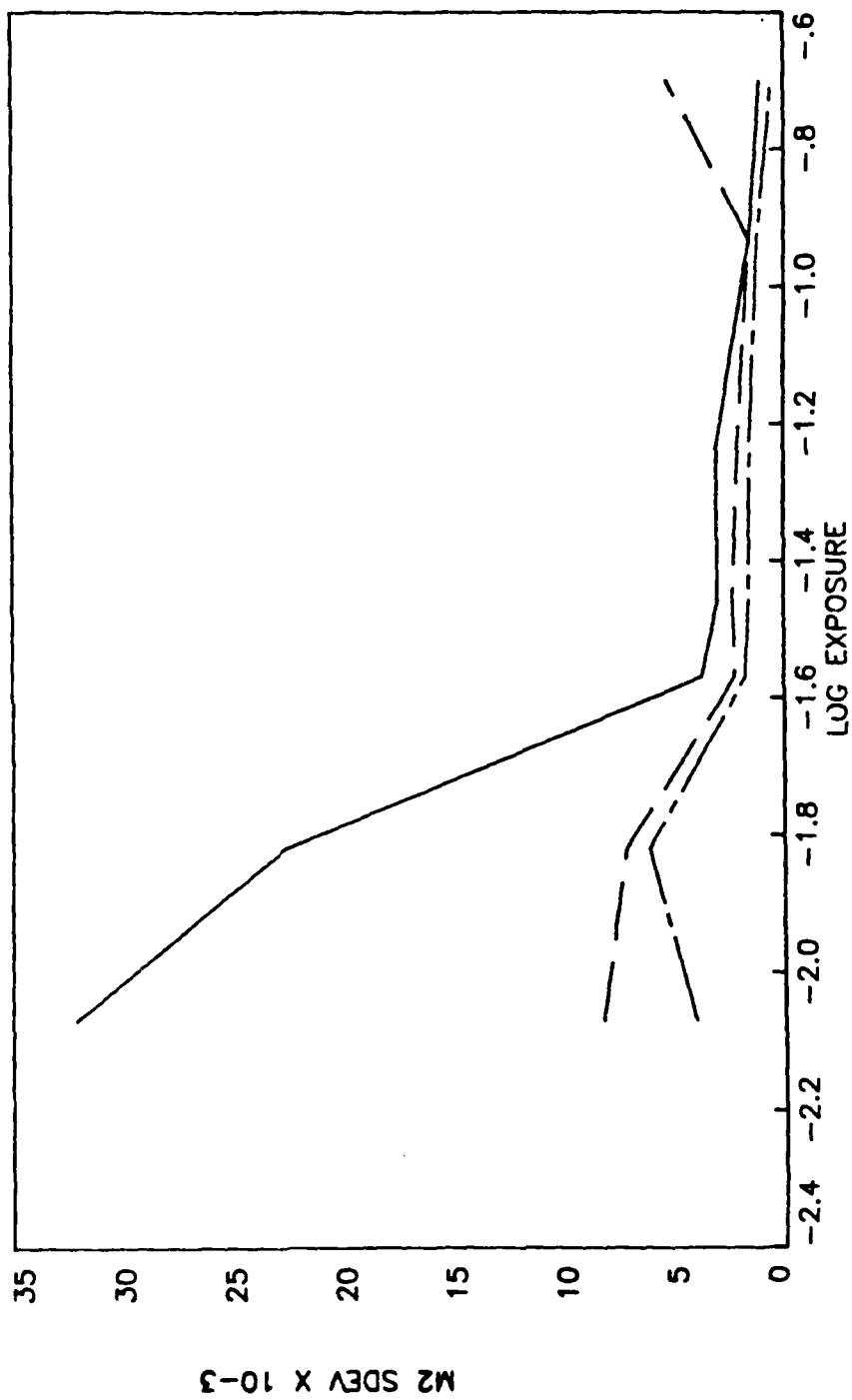


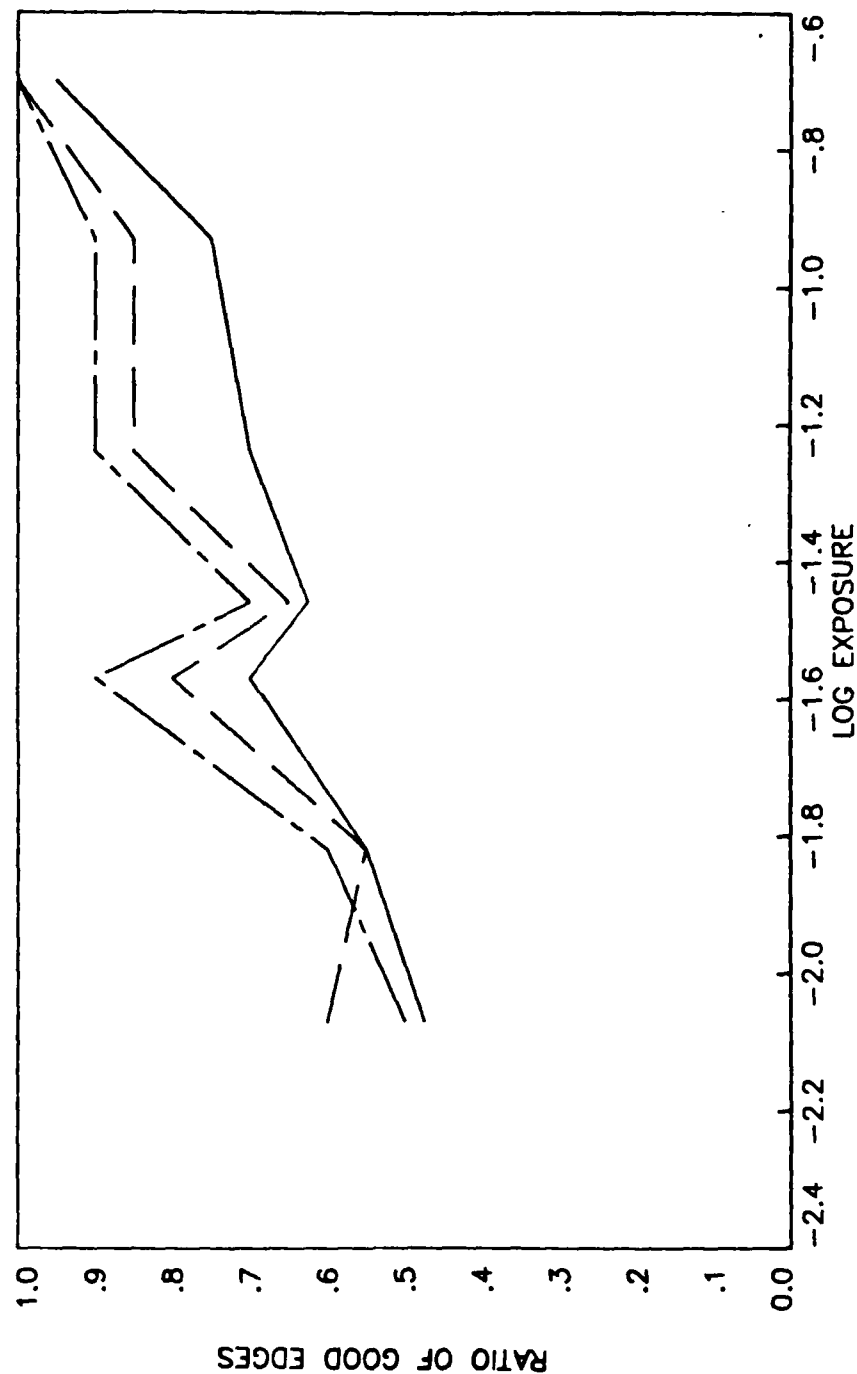
figure 24

NUMBER OF GOOD EDGES V. LOG EXPOSURE
NORMAL EXPOSURE

4 SCANS
AVERAGED

2 SCANS
AVERAGED

1 SCAN



SECOND MOMENT V. LOG EXPOSURE CPA EXPOSURE

1 SCAN

2 SCANS
AVERAGED

4 SCANS
AVERAGED

40 SCANS
AVERAGED

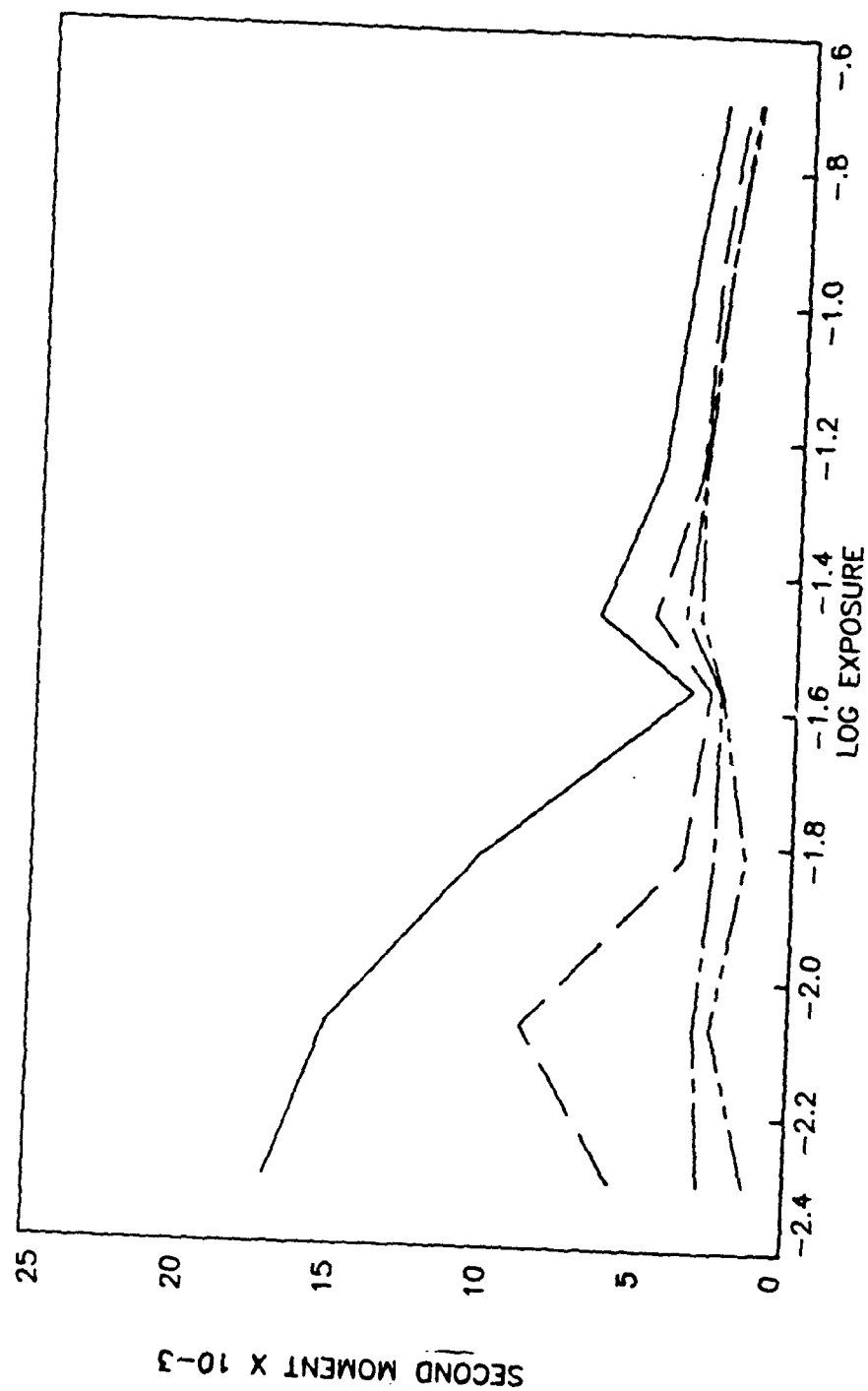
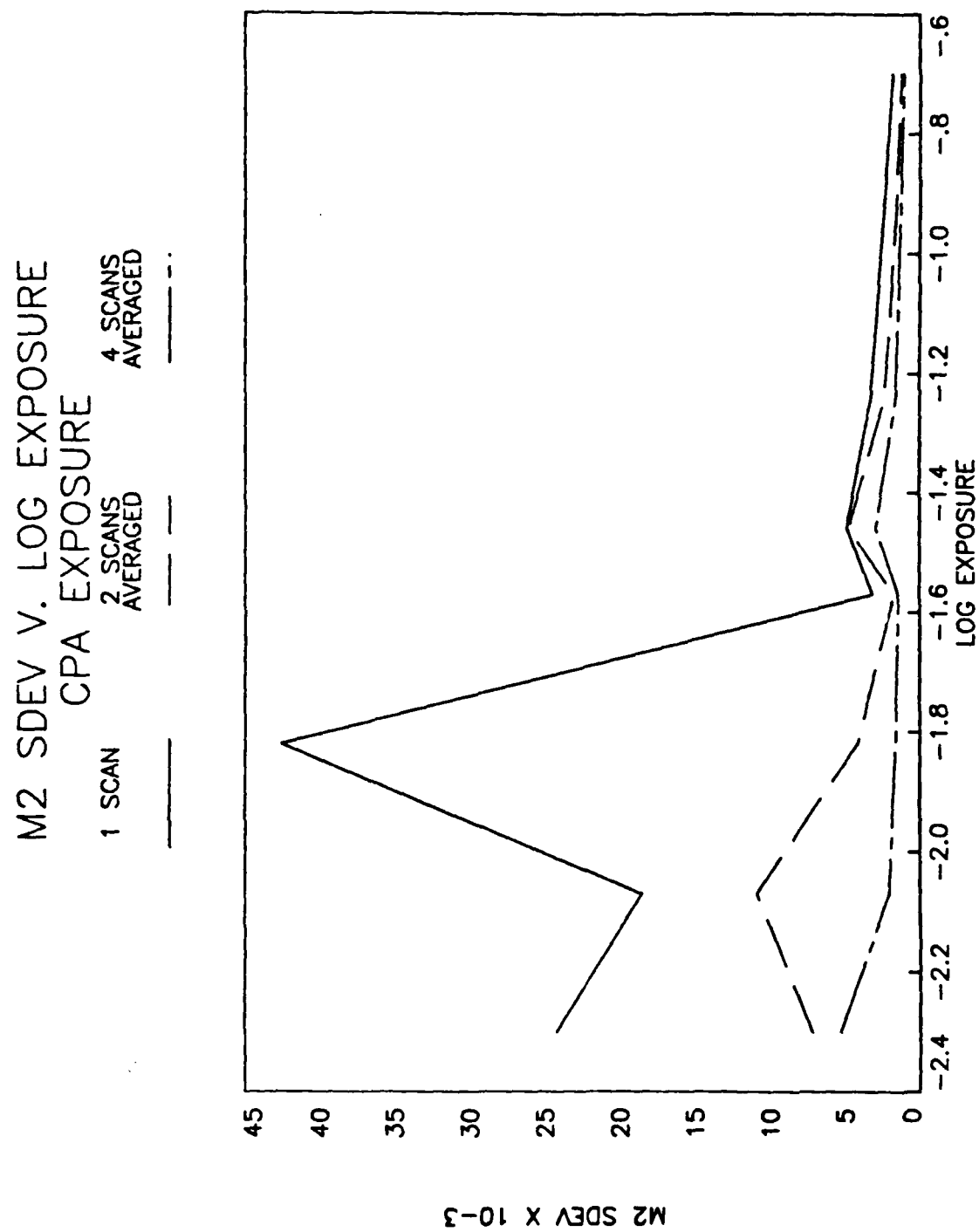


figure 25

figure 26



NUMBER OF GOOD EDGES V. LOG EXPOSURE

CPA EXPOSURE

1 SCAN

2 SCANS
AVERAGED

4 SCANS
AVERAGED

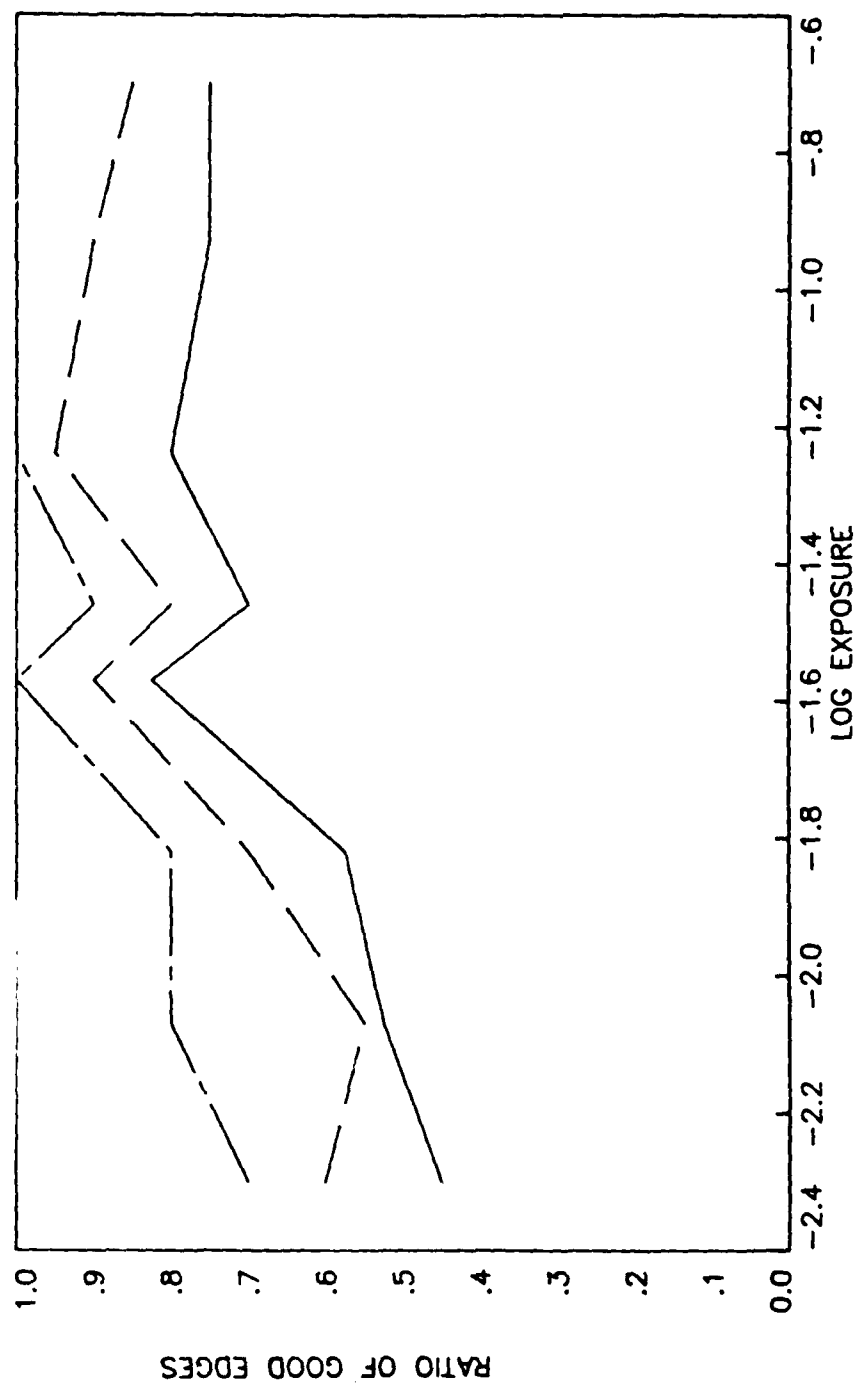


figure 27

figure 28

EDGE DIFFERENCE V. LOG EXPOSURE

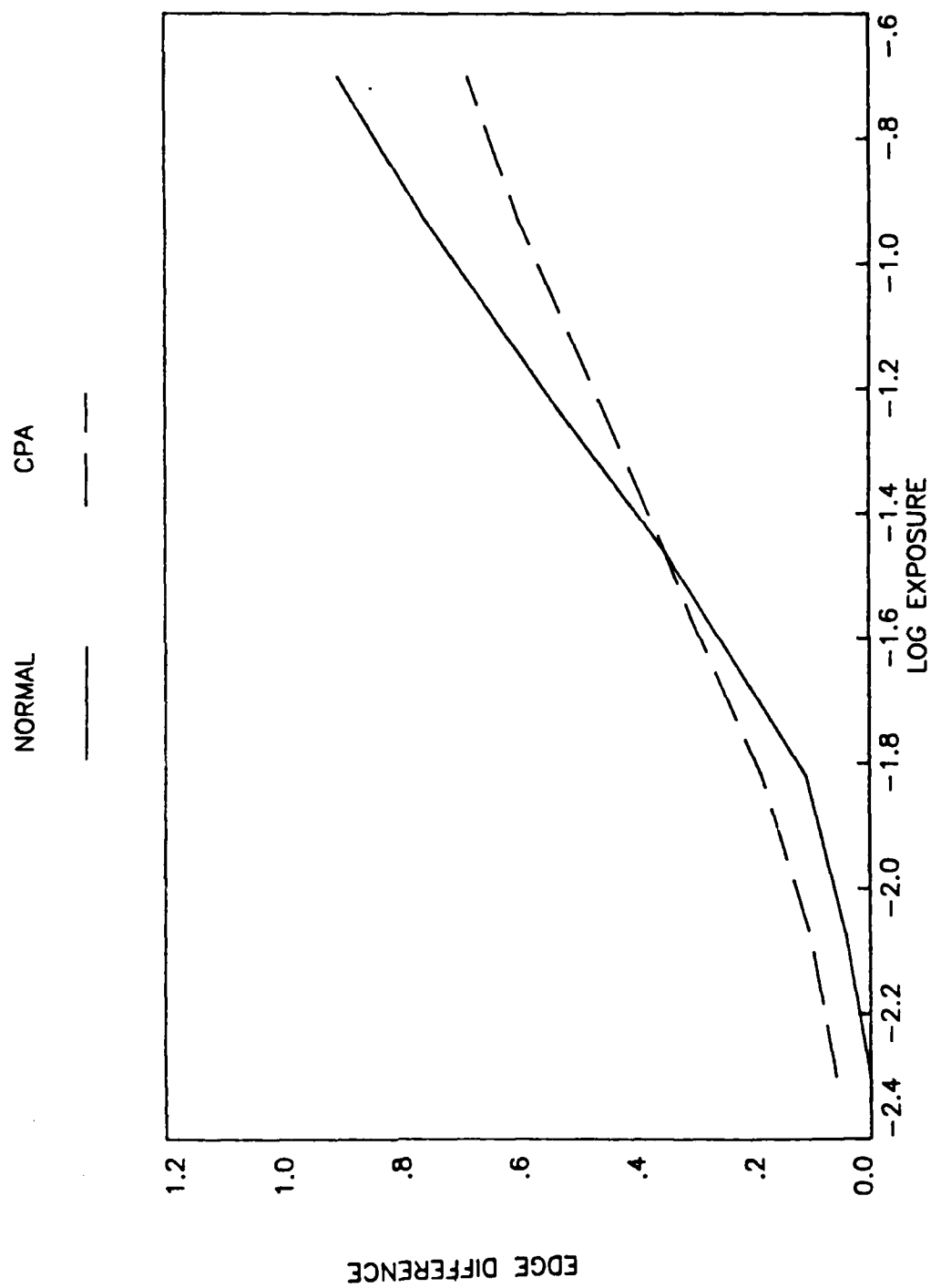


figure 29

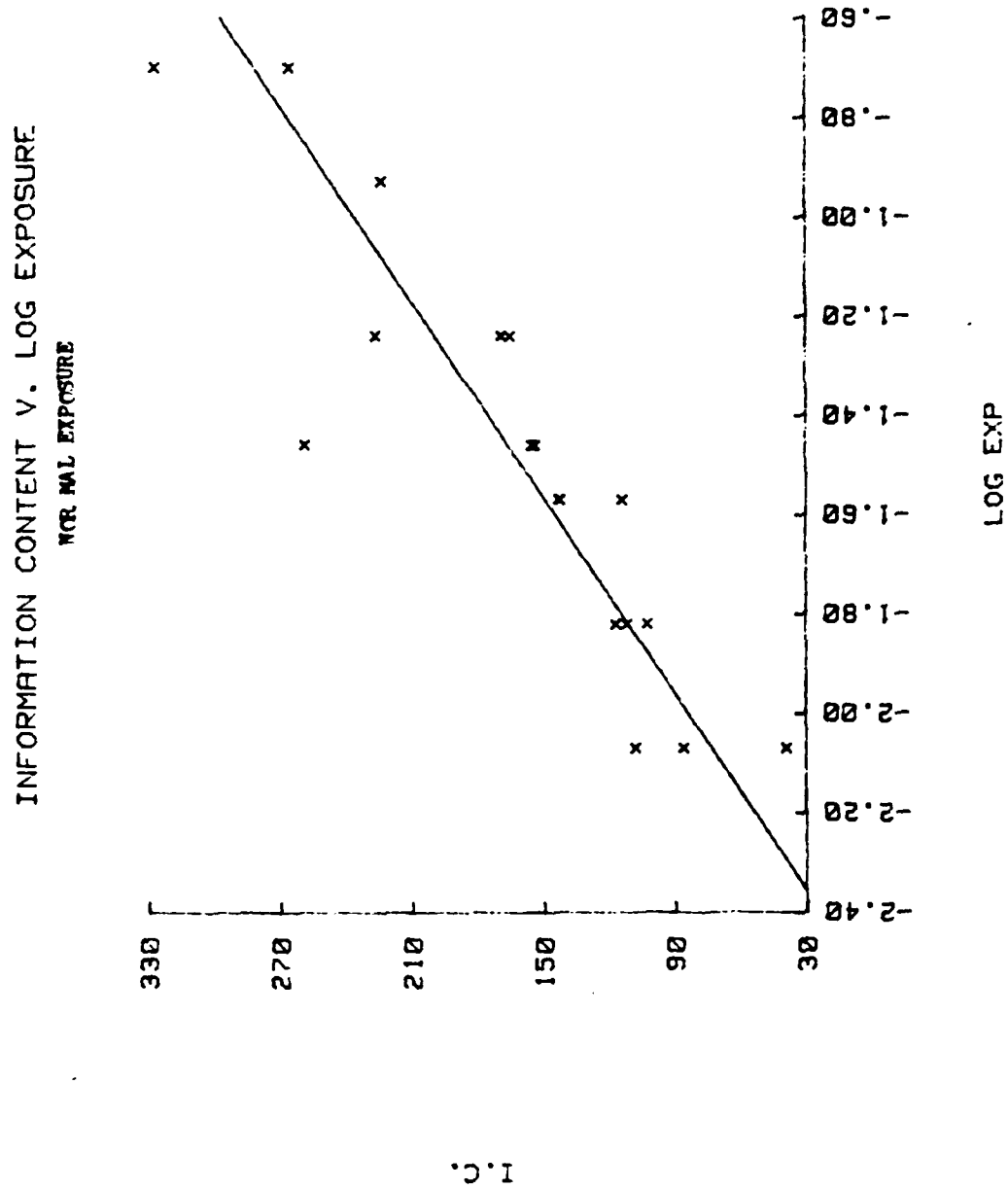
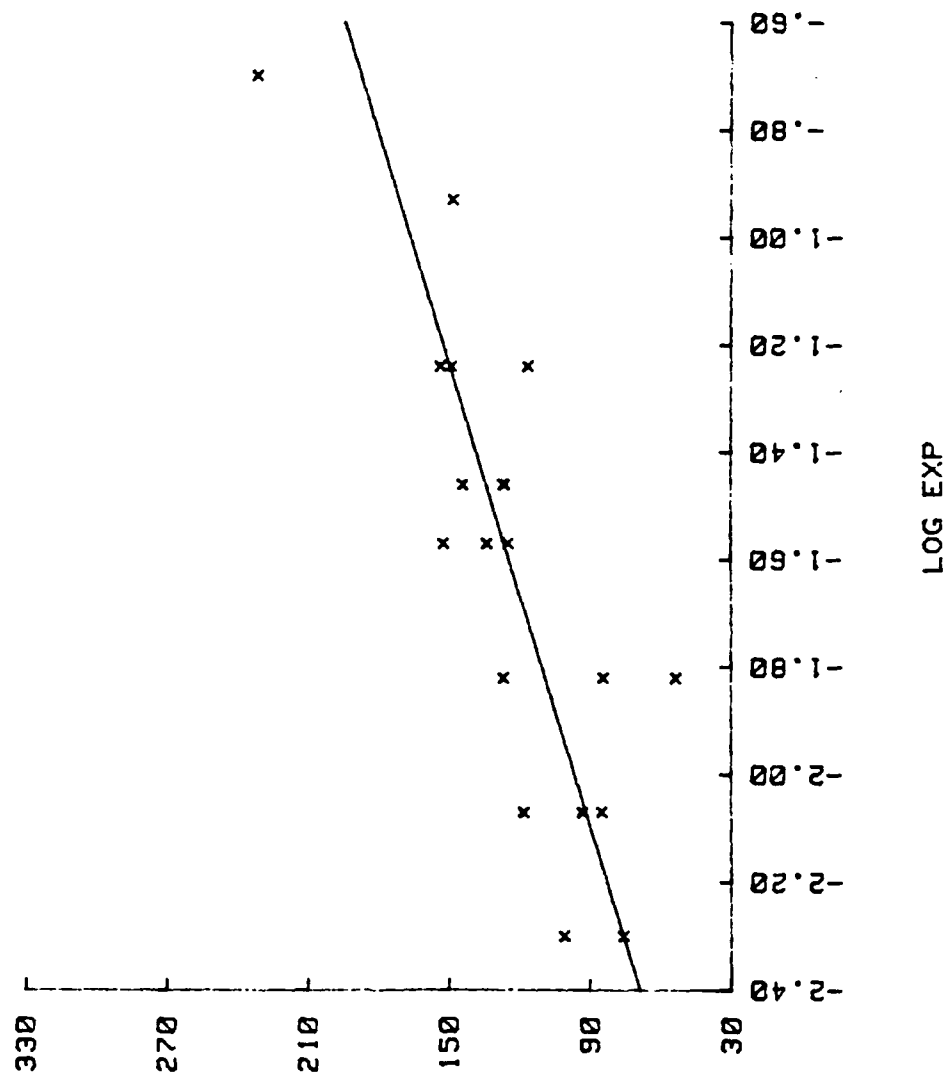


figure 30

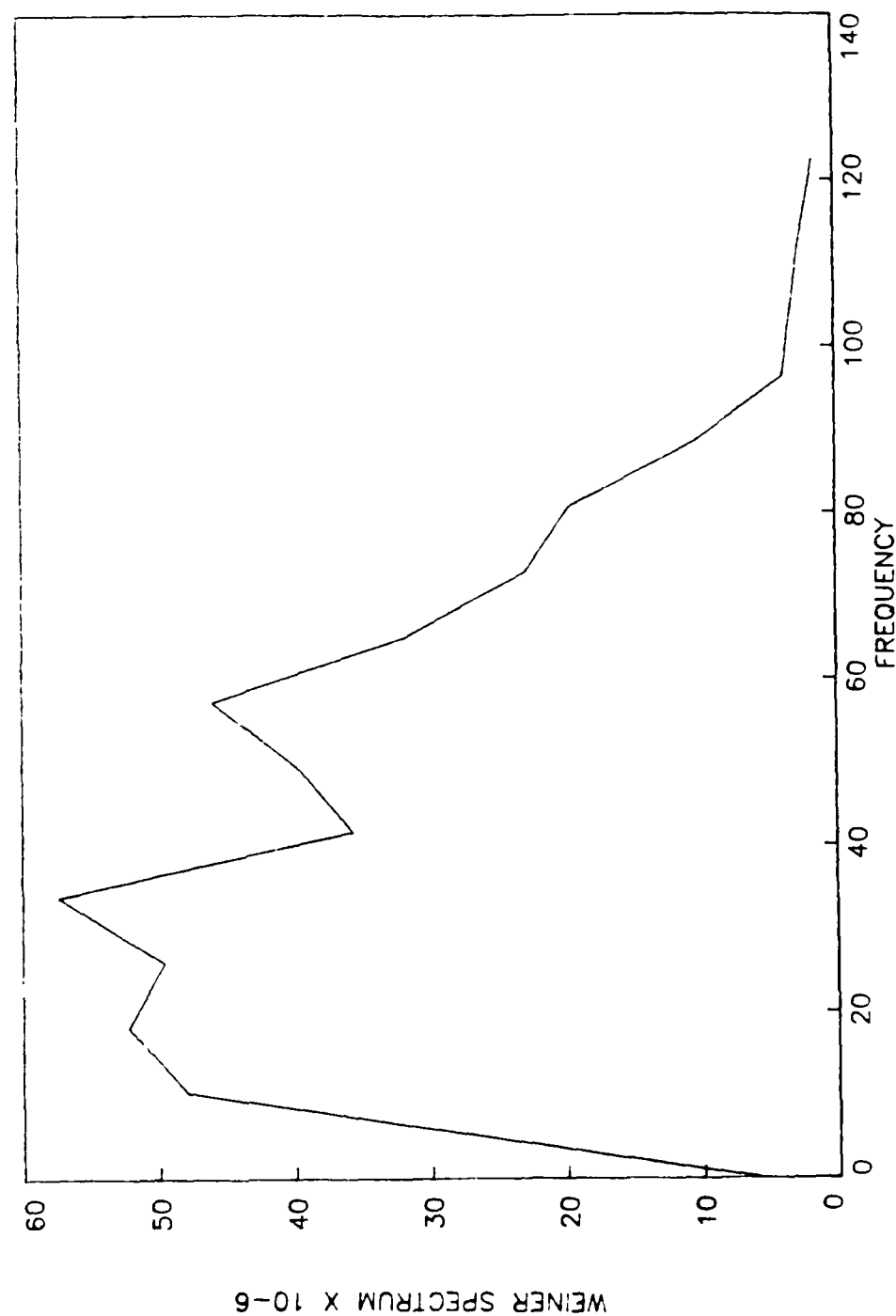
INFORMATION CONTENT V. LOG EXPOSURE
CPA EXPOSURES



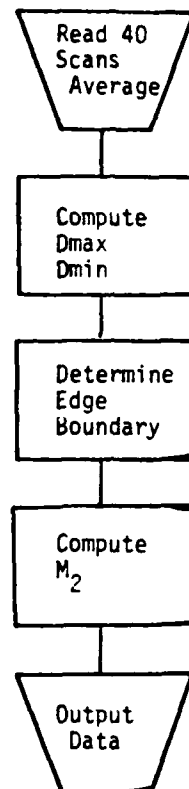
I.C.

figure 31

WEINER SPECTRUM
EXAMPLE AT -1.82 LOG EXPOSURE



Attachment 1 flow diagram



Attachment 1 code

```

C*****
C
C      CMTF.FTN   PROGRAM WRITTEN BY KONRAD KERN
C
C      THIS PROGRAM MAKES AN INITIAL LOOK AT THE DATA  AND DETERMINES THE
C      UPPER AND LOWER BOUNDS OF THE EDGE SCAN.
C
C      PROGRAM INPUTS:
C          40 EDGE SCANS OF 1024 POINTS EACH
C
C      PROGRAM OUTPUTS:
C          1. DMAX AND DMIN FOR THE 40 SCAN AVERAGED EDGE
C          2. BEGINNING, MID-POINT, AND END COORDINATES OF THE EDGE
C
C*****
      REAL*8 MRR(4), MR(40), EDGE(1024), AVE, AVL, AVH
      REAL*8 M2A, M22A, DEN(10), LE(10)
      REAL*8 AEDGE(1024), M1, M2
      INTEGER SAMPLE
      EXTERNAL FOUR1
      CALL ASSIGN(5, 'TI: ')
      CALL ASSIGN(2, 'RES DAT')
      CALL ASSIGN(1, 'EDGE DAT')
13      FORMAT(F5.2, X, F4.2)
11      FORMAT(20I4)
15      FORMAT(I3)
16      FORMAT(F5.2)
12      FORMAT(G18.10)
C BEGIN READING THE SCANS AND COMPUTING THE SECOND MOMENTS
815     FORMAT(/, 5X, 'LOG EXPOSURE=', F8.3)
802     FORMAT(/, 5X, 'SAMPLE NUMBER=', I3, 10X, 'CONTRAST=', F5.3)
803     FORMAT(/, 5X, 'EXPOSURE= ', G11.5, 5X, 'EXPOSURE TYPE= ', I3)
904     FORMAT(/, 4X, '#', 3X, 'SECOND MOMENT', 10X, 'ONE SCAN')
C PERFORM AVERAGE OF FORTY SCANS AND COMPUTE THE M2
      REWIND 1
      WRITE(5,*) 'AVERAGE OF FORTY SCANS'
      LS=0
      M2A=0.0
      M22A=0.0
C READ ALL FORTY EDGE SCANS AND AVERAGE
      DO 310 I=1, 1024
310      AEDGE(I)=0.0
           DO 321 II=1, 40
           CALL MYF(EDGE, 1024, II)
           DO 320 II=1, 1024
320      AEDGE(II)=AEDGE(II)+EDGE(II)
321      CONTINUE
           DO 331 II=1, 1024
331      EDGE(II)=AEDGE(II)/40.0
C DETERMINE DMIN OF THE EDGE
      AVE=0.0
      DO 325 II=1, 300
325      AVE=AVE+EDGE(II)
      AVE=AVE/300.0

```

Attachment 1 code, continued

```

C DETERMINE DMAX OF THE EDGE
  AVH=0.0
  DO 326 II=725,1024
326   AVH=AVH+EDGE(II)
      AVH=AVH/300.0
      AVL=AVE
C DETERMINE THE EDGE STEP DIFFERENCE
  DD=AVH-AVE
  WRITE(2,12) AVL,AVH,DD
  AVE=(AVE+AVH)/2.0
C DETERMINE THE MID POINT OF THE EDGE
  DO 327 II=1,1024
    K=II
    IF(AVE-EDGE(II)) 328,327,327
327   CONTINUE
328   CONTINUE
C DETERMINE THE END COORDINATE OF THE EDGE
  DO 350 II=1,1024
    IF(AVH-EDGE(II)) 355,355,350
350   CONTINUE
355   LH=II+3
C DETERMINE THE BEGINNING COORDINATE OF THE EDGE
  DO 360 II=1,LH
    LL=LH-II
    IF(EDGE(LL)-AVL) 365,365,360
360   CONTINUE
365   LL=LL-3
    DO 390 I=LL,LH
      J=I-LL+1
390   EDGE(J)=EDGE(I)
      K=K-LL
C COMPUTE THE SECOND MOMENT OF THE EDGE
  CALL SECMD(EDGE,M1,M2,AVL,AVH,J,K)
  LS=1
  JK=LH-LL
  WRITE(2,15) LL,K,LH
  WRITE(2,12) M1
850   FORMAT(1X,'LL=',I4,3X,'SPREAD=',I4,3X,'LH=',I4)
      WRITE(5,800) LS,M1,M2
800   FORMAT(1X,I3,3X,'M1=',G15.5,3X,'M2=',G15.5)
500   FORMAT(3X,G15.5,3X,I4)
810   FORMAT(/,5X,'EDGE DENSITY CHANGE=',G10.5,5X,'NOISE SDEV=',G10.5)
999   STOP
      END
C SECOND MOMENT SUBROUTINE
  SUBROUTINE SECMD(EDGE,M1,M2,AVL,AVH,J,K)
  REAL*8 EDGE(1024),ALINE(100),M1,M2
  REAL*8 AM1,AM2,AVL,AVH
  AM2=0.0
  AM1=0.0
  IF(AVH-AVL) 800,800,3
  DO 10 I=1,J
10    EDGE(I)=(EDGE(I)-AVL)/(AVH-AVL)

```

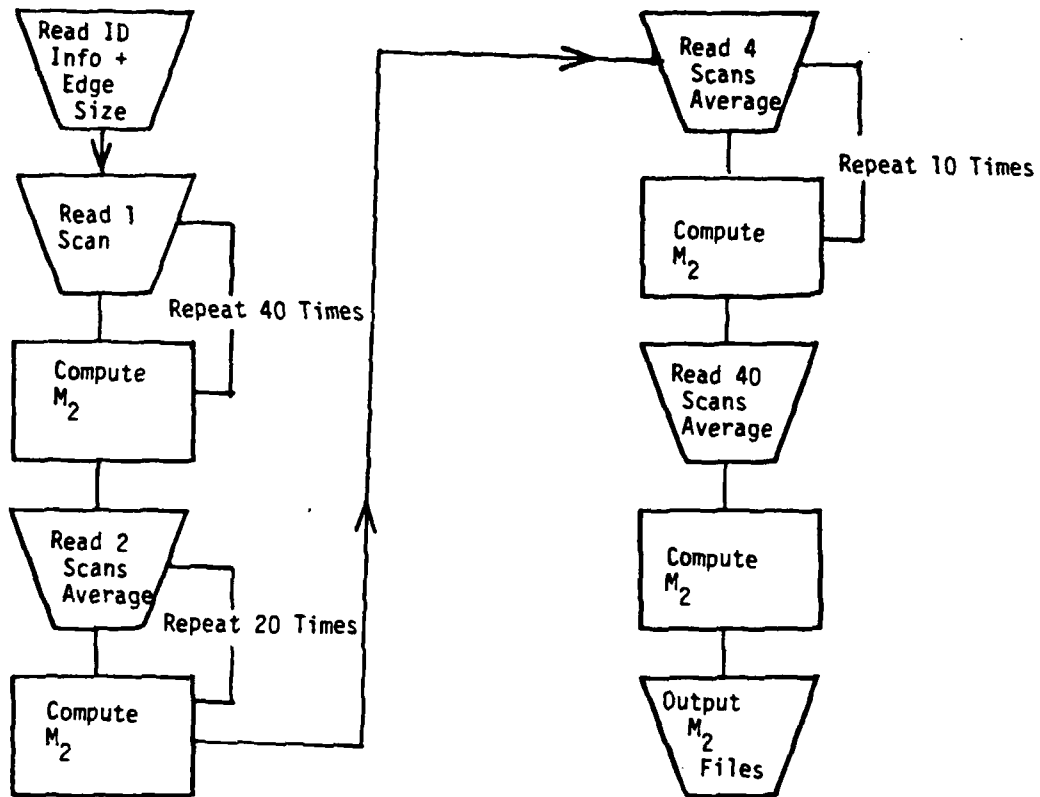
Attachment 1 code, continued

```

C CALCULATE M1
  DO 50 I=2,J
    S=I-1
50   AM1=AM1+(EDGE(I)-EDGE(I-1))*(S*0.003+0.0015)
    WRITE(5,*) 'CALCULATED M1',AM1
C CALCULATE M2 THE FIRST TIME
  DO 60 I=2,J
    S=I-1
60   AM2=AM2+(EDGE(I)-EDGE(I-1))*((0.003*S-AM1+0.0015)**2)
    GOTO 810
800  M2=-100
    GOTO 820
810  M1=AM1
    M2=AM2
820  RETURN
    END
C SUBROUTINE TO READ THE EDGE SCANS
  SUBROUTINE MYF(VAL,N,LF)
    INTEGER EDGE(1024)
    REAL*8 VAL(1024)
    CHARACTER*80 HEAD(3)
    READ(LF,900) (HEAD(I),I=1,3)
900  FORMAT(A80)
    READ(LF,901) (EDGE(J),J=1,N)
    DO 10 J=1,N
10   VAL(J)=EDGE(J)/1000.0
901  FORMAT(20I4)
902  FORMAT(1X,20I4)
    RETURN
  END

```


Attachment 2 flow diagram



Attachment 2 code

```

C*****
C
C      MTF.FTN      PROGRAM WRITTEN BY KONRAD KERN
C
C      PROGRAM INPUTS:
C          1. DMAX AND DMIN VALUES FOR THE TOTAL AVERAGED EDGE
C             COMPUTED IN FORMER PROGRAM
C          2. EDGE BEGINNING, MID-POINT, AND END ARRAY COORDINATES
C          3. 40 ARRAYS OF EDGE SCAN DATA, 1024 SAMPLE POINTS EACH
C
C      PROGRAM OUTPUTS:
C          1. M2 VALUES COMPUTED USING SINGLE SCAN VALUES, STATISTICS
C          2. M2 VALUES COMPUTED USING AVERAGES OF 2 SCANS, STATISTICS
C          3. M2 VALUES COMPUTED USING AVERAGES OF 4 SCANS, STATISTICS
C          4. M2 VALUE COMPUTED USING AVERAGE OF 40 SCANS
C*****

      REAL*8 MRR(4), MR(40), EDGE(1024), AVE, AVL, AVH
      REAL*8 M2A, M22A, LS, DEN(10), LE(10)
      REAL*8 AEDGE(1024), M1, M2
      INTEGER SAMPLE
      EXTERNAL FOUR1
      CALL ASSIGN(5, 'TI: ')
      CALL ASSIGN(4, 'RES.DAT')
      CALL ASSIGN(2, 'MRES.DAT')
      CALL ASSIGN(1, 'EDGE.DAT')
13      FORMAT(F5.2, X, F4.2)
11      FORMAT(20I4)
15      FORMAT(I3)
16      FORMAT(F5.2)
C SAMPLE IDENTIFICATION INFORMATION
      WRITE(5,*) 'SAMPLE NUMBER ?'
      READ(5,15) SAMPLE
      WRITE(5,*) 'NORMAL=1, CPA=2'
      READ(5,15) IDS
      WRITE(5,*) 'LOG EXPOSURE=?'
      READ(5,12) EXL
C READ IN DATA FROM FORMER PROGRAM
      READ(4,12) AVL
      WRITE(5,*) AVL
      READ(4,12) AVH
      WRITE(5,*) AVH
      READ(4,12) DD
      WRITE(5,*) DD
      READ(4,15) LL
      WRITE(5,*) LL
      READ(4,15) K
      WRITE(5,*) K
      READ(4,15) LH
      WRITE(5,*) LH
      READ(4,12) M1
12      FORMAT(G18.10)

```

Attachment 2 code, continued

```

C BEGIN READING THE SCANS AND COMPUTING THE SECOND MOMENTS
  WRITE(2,802) SAMPLE, CON
  WRITE(2,815) EXL
815  FORMAT(/,5X,'LOG EXPOSURE=',F8.3)
802  FORMAT(/,5X,'SAMPLE NUMBER=',I3,10X,'CONTRAST=',F5.3)
  WRITE(2,803) QA, IDS
803  FORMAT(/,5X,'EXPOSURE= ',G11.5,5X,'EXPOSURE TYPE= ',I3)
  WRITE(2,904)
904  FORMAT(/,4X,'*',3X,'SECOND MOMENT',10X,'ONE SCAN')
C SINGLE SCAN DATA COMPUTATIONS OF M2
24  LS=0
    M2A=0.0
    M22A=0.0
    DO 20 I=1,40
      CALL MYF(EDGE,1024,1)
    DO 37 II=LL,LH
      J=II-LL+1
137  EDGE(J)=EDGE(II)
    CALL SECMD(EDGE,M1,M2,AVL,AVH,J,K)
    IF(M2) 20,20,29
29  LS=LS+1
    M2A=M2A+M2
    M22A=M22A+M2*M2
    MR(LS)=M2
  WRITE(5,800)LS,M1,M2
800  FORMAT(1X,F4.1,5X,' M1= ',1X,G11.5,5X,' M2= ',1X,G11.5)
20  CONTINUE
  WRITE(2,804) (J,MR(J),J=1,LS)
804  FORMAT(1X,I4,5X,G11.5)
    IF(LS-2.0) 31,32,32
32  D=SQRT(ABS(LS*M22A-M2A**2)/(LS*(LS-1)))
    M2A=M2A/LS
31  WRITE(2,805) M2A,D
805  FORMAT(/,5X,'AVERAGED M2= ',G11.5,5X,'SDEV = ',G11.5)
10  CONTINUE
C PERFORM AVERAGE OF TWO SCANS AND RECOMPUTE THE M2
  REWIND 1
  WRITE(2,905)
905  FORMAT(/,4X,'*',3X,'SECOND MOMENT',10X,'TWO SCANS')
    LS=0
    M2A=0.0
    M22A=0.0
    DO 120 I=1,20
      CALL MYF(EDGE,1024,1)
    DO 131 II=1,1024
      AEDGE(II)=EDGE(II)
131  CALL MYF(EDGE,1024,1)
    DO 132 II=1,1024
132  EDGE(II)=(AEDGE(II)+EDGE(II))/2.0
    DO 137 II=LL,LH
      J=II-LL+1
137  EDGE(J)=EDGE(II)

```

Attachment 2 code, continued

```

CALL SECMD(EDGE, M1, M2, AVL, AVH, J, K)
  IF (M2) 120, 120, 129
129   LS=LS+1
      M2A=M2A+M2
      M22A=M22A+M2**2
      WRITE(5, 800) LS, M1, M2
      MR(LS)=M2
120   CONTINUE
      WRITE(2, 804) (J, MR(J), J=1, LS)
      IF (LS-2, 0) 130, 133, 133
133   D=SQRT(ABS(LS*M22A-M2A**2)/(LS*(LS-1)))
      M2A=M2A/LS
130   WRITE(2, 805) M2A, D
C     AVERAGE FOUR EDGES AND COMPUTE SECOND MOMENT
      REWIND 1
      WRITE(2, 906)
906   FORMAT(////////, 4X, '#', 3X, 'SECOND MOMENT', 10X, 'FOUR SCANS')
      LS=0
      M2A=0.0
      M22A=0.0
      DO 220 I=1, 10
      CALL MYF(EDGE, 1024, 1)
      DO 221 II=1, 1024
221   AEDGE(II)=EDGE(II)
      CALL MYF(EDGE, 1024, 1)
      DO 222 II=1, 1024
222   AEDGE(II)=EDGE(II)+AEDGE(II)
      CALL MYF(EDGE, 1024, 1)
      DO 223 II=1, 1024
223   AEDGE(II)=EDGE(II)+AEDGE(II)
      CALL MYF(EDGE, 1024, 1)
      DO 224 II=1, 1024
224   EDGE(II)=(EDGE(II)+AEDGE(II))/4.0
      DO 237 II=LL, LH
      J=II-LL+1
237   EDGE(J)=EDGE(II)
      CALL SECMD(EDGE, M1, M2, AVL, AVH, J, K)
      IF (M2) 220, 220, 229
229   LS=LS+1
      M2A=M2A+M2
      M22A=M22A+M2**2
      MR(LS)=M2
      WRITE(5, 800) LS, M1, M2
220   CONTINUE
      WRITE(2, 804) (J, MR(J), J=1, LS)
      IF (LS-2, 0) 231, 232, 232
232   D=SQRT(ABS(LS*M22A-M2A**2)/(LS*(LS-1)))
      M2A=M2A/LS
231   WRITE(2, 805) M2A, D
C     PERFORM AVERAGE OF FORTY SCANS AND RECOMPUTE THE M2
      REWIND 1
      WRITE(2, *) 'AVERAGE OF FORTY SCANS'
      WRITE(5, *) 'AVERAGE OF FORTY SCANS'
      LS=0
      M2A=0.0

```

Attachment 2 code, continued

```

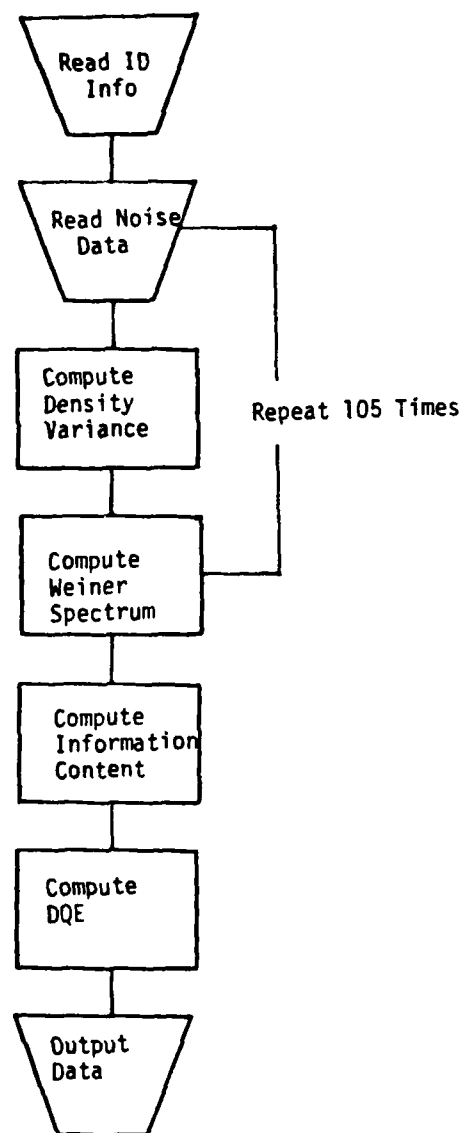
      M22A=0.0
      DO 310 I=1,1024
310    AEDGE(I)=0.0
        DO 321 I=1,40
          CALL MYF(EDGE,1024,I)
          DO 320 II=1,1024
320    AEDGE(II)=AEDGE(II)+EDGE(II)
321    CONTINUE
        DO 331 II=1,1024
331    EDGE(II)=AEDGE(II)/40.0
        DO 337 II=LL,LH
          J=II-LL+1
337    EDGE(J)=EDGE(II)
          CALL SECMD(EDGE,M1,M2,AVL,AVH,J,K)
          IF(M2) 341,340,340
341    M2=ABS(M2)
        M1=-1000.0
340    D=0.0
        LS=1.0
        WRITE(5,800) LS,M1,M2
        WRITE(2,800) LS,M1,M2
        WRITE(2,810) DD,SDD
        WRITE(5,810) DD,SDD
810    FORMAT(/,5X,'EDGE DENSITY CHANGE=',G10.5,5X,'NOISE SDEV=',G10.5)
999    STOP
      END
C SECOND MOMENT SUBROUTINE
      SUBROUTINE SECMD(EDGE,M1,M2,AVL,AVH,J,K)
      REAL*8 EDGE(1024),ALINE(100),X,Y,M1,M2
      REAL*8 AM1,AM2
      AM2=0.0
      AM1=0.0
      IF(AVH-AVL) 800,800,5
5      DO 10 I=1,J
10      EDGE(I)=(EDGE(I)-AVL)/(AVH-AVL)
C CALCULATE L(X)
C CALCULATE M1
      DO 40 I=2,J
        S=I-1
40      AM1=AM1+(EDGE(I)-EDGE(I-1))*S*0.003
        WRITE(5,*)'CALCULATED M1',AM1
C CALCULATE M2 THE FIRST TIME
      DO 60 I=2,J
        S=I-1
60      AM2=AM2+(EDGE(I)-EDGE(I-1))*((0.003*S-AM1+0.0015)**2)
      GOTO 810
800    M2=-100
      GOTO 820
810    M2=AM2
820    RETURN
      END

```

Attachment 2 code, continued

```
SUBROUTINE MYF(VAL, N, LF)
  INTEGER EDGE(1024)
  REAL*8 VAL(1024)
  CHARACTER*80 HEAD(3)
  READ(LF, 900) (HEAD(I), I=1, 3)
900  FORMAT(A80)
  READ(LF, 901) (EDGE(J), J=1, N)
  DO 10 J=1, N
10   VAL(J)=EDGE(J)/1000.0
901  FORMAT(20I4)
902  FORMAT(1X, 20I4)
  RETURN
END
```

Attachment 3 flow diagram



Attachment 3 code

```

C *****
C
C   THE FOR    PROGRAM WRITTEN BY KONRAD KERN
C
C   PROGRAM INPUTS
C       1. SECOND MOMENT, COMPUTED IN FORMER PROGRAM
C       2. EDGE STEP, COMPUTED IN FORMER PROGRAM
C       3. NOISE SCAN DATA, 105 BLOCKS OF 64 SAMPLES
C       4. EXPOSURE IRRADIANCE IN PHOTONS PER CM**2
C       5. CONTRAST
C       6. SAMPLE DATA IDENTIFICATION
C
C   PROGRAM OUTPUTS:
C       1. DENSITY VARIANCE
C       2. DGE
C       3. WEINER SPECTRUM
C       4. INFORMATION CONTENT
C *****
C
C       REAL*8 D2(105),NOST(64)
C       REAL*8 NOISE(128)
C       REAL*8 IC(64),MTF(64),LS,DEN(10),LE(10)
C       REAL*8 WS(128),B,C,D2BAR,M1,M2
C       COMPLEX NS(128),NSC(128)
C       INTEGER SAMPLE
C       COMMON DEN,LE
C       EXTERNAL FOUR1
C       CALL ASSIGN(5,'TI:')
C       CALL ASSIGN(2,'RES DAT')
C       CALL ASSIGN(3,'NOIS.DAT')
13       FORMAT(F5.2,X,F4.2)
11       FORMAT(20I4)
15       FORMAT(I3)
16       FORMAT(F5.2)
C SAMPLE IDENTIFICATION INFORMATION
C       WRITE(5,*) 'SAMPLE NUMBER ?'
C       READ(5,15) SAMPLE
C       WRITE (5,*) 'NORMAL=1,CPA=2'
C       READ(5,15)IDS
C       WRITE (5,*) 'IMAGE CONTRAST'
C       READ(5,12) CON
C       WRITE(5,*) 'LOG EXPOSURE=?'
C       READ(5,12) EXL
C       WRITE(5,*) 'EXPOSURE IN PHOTONS/AREA'
C       READ(5,12) QA
C EDGE STEP AND M2 COMPUTED IN FORMER PROGRAM
C       WRITE(5,*) 'EDGE STEP'
C       READ(5,12)DD
C       WRITE(5,*) 'TOTAL M2'
C       READ(5,12)M2
C       AREA=731.6E-9
12       FORMAT(G10.5)
C       WRITE(2,802) SAMPLE, CON

```


Attachment 3 code, continued

```

      WRITE(2,815) EXL
815   FORMAT(/,5X,'LOG EXPOSURE=',F8.3)
802   FORMAT(/,5X,'SAMPLE NUMBER=',I3,10X,'CONTRAST=',F5.3)
      WRITE(2,803) QA, IDS
      WRITE(2,850)M2
850   FORMAT(5X,'M2 USED=',G10.5)
803   FORMAT(/,5X,'EXPOSURE= ',G11.5,5X,'EXPOSURE TYPE= ',I3)
C BEGIN COMPUTING THE NOISE INFORMATION
      DO 400 I=1,128
        WS(I)=0.0
400   D2(I)=0.0
        D2BAR=0.0
        DO 540 J=1,105
          CALL MYF(NOST,64,3)
          B=0.00
          C=0.00
C COMPUTE DENSITY VARIANCE
          DO 550 I=1,64
            NOISE(I)=NOST(I)
            B=B+NOST(I)
            C=C+NOST(I)*NOST(I)
550     CONTINUE
          D2(J)=ABS(64.0*C-B*B)/(64.0*63.0)
          D2BAR=D2BAR+D2(J)
          WRITE(5,901)J, D2(J), D2BAR
901   FORMAT(1X, I5, 2X, 'D2=', 1X, G11.5, 3X, 'D2BAR=', 1X, G11.5)
C REMOVE DC LEVEL
      A=0.0
      DO 570 I=1,64
570   A=A+NOISE(I)
      A=A/64.0
      DO 580 I=1,64
580   NOISE(I)=NOISE(I)-A
C APPLY BARTLETT WINDOW
      DO 590 I=1,32
590   NS(I)=CMPLX(NOISE(I)*(1.0-1.0/32.0*I))
      DO 591 I=1,32
591   NS(129-I)=CMPLX(NOISE(I+32)*(1.0-1.0/32.0*I))
      DO 600 I=33,96
600   NS(I)=(0.0,0.0)
C TRANSFORM TO FREQUENCY
      CALL FOUR1(NS,128,1)
      DO 610 I=1,128
610   NSC(I)=CONJG(NS(I))
      NOISE(I)=(CABS(NS(I)*NSC(I)))*2
C PERFORM ENSEMBLE AVERAGE OF WEINER SPECTRUM
      DO 630 I=1,128
630   WS(I)=WS(I)+NOISE(I)
640   CONTINUE
C AVERAGE WEINER SPECTRUM AND PERFORM FFT SCALING
      DO 640 I=1,128
640   WS(I)=WS(I)/105.0/128.0
      D2BAR=D2BAR/105.0
      SDD=SQRT(D2BAR)
      AL2=ALOG(2.0)

```

Attachment 3 code, continued

```

C COMPUTE FIRST MOMENT OF WEINER SPECTRUM
  M1=0.0
  DO 650 I=2,64
    S=I-1.
650    M1=M1+(WS(I)-WS(I-1))*S*2.604
    WRITE(2,806) M1
806    FORMAT(/,5X,'WEINER SPECTRUM M1 = ',G11.5)
    WRITE(2,903)
903    FORMAT(/,10X,'WEINER SPECTRUM',/)
    WRITE(2,902) (WS(I),I=1,64)
902    FORMAT(1X,G11.5,5X,G11.5,5X,G11.5)
C COMPUTE INFORMATION CONTENT
  SUM=0.0
  B=1.666**2
  A=DD**2/4.0
  DO 660 I=1,64
    F=FLOAT(I-1)*2.604
    MTF(I)=1-2.0*3.1416**2*F**2*M2
    IF (MTF(I)) 656,656,658
656    MTF(I)=0.0
658    P=A/(B+F**2)
    Q=1.0+P*(MTF(I)/WS(I))
660    IC(I)=ALOG(Q)/AL2*F
C INTEGRATION BY SIMPSON'S RULE
  DO 670 I=2,64
670    SUM=SUM+(IC(I)+IC(I-1))/2.0*2.604
    SUM=SUM*3.1416
C OUTPUT CALCULATED VALUES
  WRITE(2,810) DD,SDD
810    FORMAT(/,5X,'EDGE DENSITY CHANGE=',G10.5,5X,'NOISE SDEV=',G10.5)
    WRITE(2,807) SUM
807    FORMAT(/,5X,'INFORMATION CAPACITY = ',G11.5)
    DGE=0.1886*CON*CON/(GA*AREA*D2BAR)
950    FORMAT(G16.5)
    WRITE(2,808) AREA,D2BAR,DGE
808    FORMAT(/,2X,'AREA=',G11.5,3X,'D2=',G11.5,3X,'DGE=',G11.5,///)
999    STOP
    END
  SUBROUTINE MYF(VAL,N,LF)
    INTEGER IEDGE(1024)
    REAL*8 VAL(1024)
    CHARACTER*80 HEAD(3)
    READ(LF,900) (HEAD(I),I=1,3)
900    FORMAT(A80)
    READ(LF,901) (IEDGE(J),J=1,N)
    DO 10 J=1,N
      VAL(J)=IEDGE(J)
10    VAL(J)=VAL(J)/1000.0
901    FORMAT(2014)
902    FORMAT(1X,2014)
    RETURN
  END

```

AD-A151 831

A QUANTITATIVE IMAGE EVALUATION STUDY OF A CONCURRENT
PHOTON AMPLIFICATION TREATED EMULSION(U) AIR FORCE INST
OF TECH WRIGHT-PATTERSON AFB OH K E KERN 1984

2/2

UNCLASSIFIED

AFIT/CI/NR-85-8T

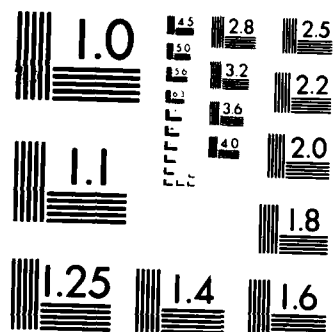
F/G 14/5

NL

END

7/10/85

END



MICROCOPY RESOLUTION TEST CHART
NATIONAL BUREAU OF STANDARDS-1963-A

VITA

Konrad E. Kern was born 8 May 1953 in Seattle, Washington. Primarily raised and educated in Honolulu, Hawaii, he received a B.A. degree in chemistry from the University of Hawaii in 1974. That same year he was commissioned an officer in the United States Air Force where he has served to date. Most of his professional life was flying until selected for post-graduate education under the sponsorship of the Air Force Institute of Technology. This thesis represents the final requirement of that post graduate education.

END

FILMED

5-85

DTIC